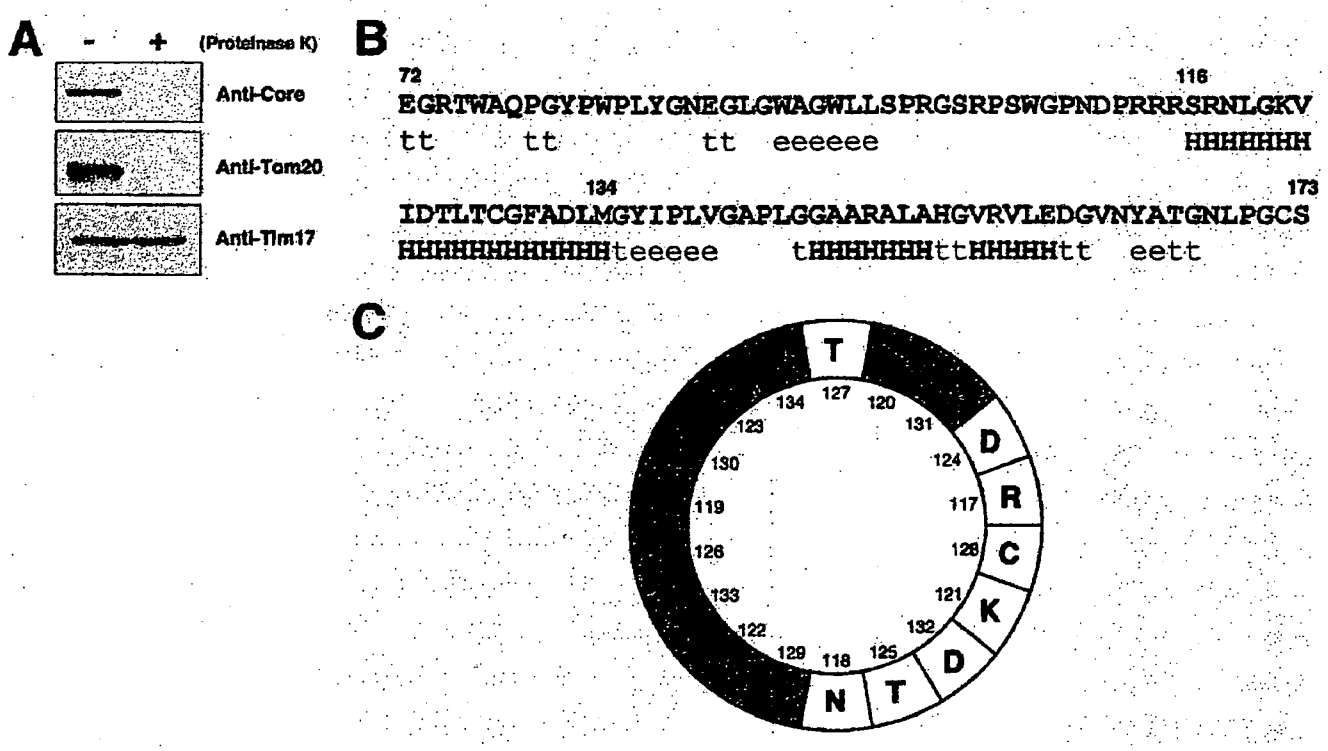


FIG. 6. (A) Protease protection assay. A mitochondrial fraction isolated from cells expressing the core protein was treated with proteinase K (+) as described in Materials and methods. The sample as well as the nontreated fraction (−) were subjected to immunoblotting with a monoclonal antibody against either HCV core, Tom20, or Tim17. (B) Protein sequence and predicted secondary structure of HCV core, amino acids 72 to 173. The secondary structure prediction was obtained with the self-optimized prediction method, a computer program on the internet (http://npsa-pbil.ibcp.fr/cgi-bin/npsa_automat.pl?page = /NPSA/npsa_sopm.html). H, α-helix; t, turn; e, extension. (C) α-Helical plot of amino acids 117 to 134 of the core protein. In the helical wheel plots, the gray shading represents apolar and hydrophobic residues; and the white represents polar residues.

protein expressed by the wild-type and NLS mutants (Fig. 7D). As expected, a fusion protein containing wild-type core protein (amino acids 1 to 71) and GFP was localized exclusively to the nucleus. Core proteins from three fusion proteins containing substitutions in each NLS motif (NLS/m1, NLS/m2, and NLS/m3) were detected primarily in the nucleus. Weak fluorescence was also observed in the cytoplasm, suggesting that these mutations caused a slight reduction in the efficiency of nuclear translocation. On the other hand, two or three NLS motif substitution mutations (NLS/m4, NLS/m5, NLS/m6, and NLS/m7) completely abolished nuclear translocation, resulting in a diffuse distribution of core protein, similar to that of GFP alone. Although it is likely that all three putative NLS motifs play a role, the above results suggest that at least two of the three putative NLS motifs are prerequisite for efficient nuclear translocation of the core protein.

## DISCUSSION

HCV core protein is released from the viral polyprotein by a host protease(s) within the ER membrane at a signal peptide sequence lying between the core and envelope (E1) proteins (16, 41). Subsequently, the signal peptide is further processed by an intramembranous protease called signal peptide peptidase (38, 53). This mature form of the core protein is then released and undergoes subcellular trafficking (30, 53). The core protein localizes mainly to the ER, mitochondria, and lipid droplets. Some reports also describe localization of the core protein to the nuclei of hepatocytes in HCV-infected patients (10), transgenic mice (34), and cultured cells expressing viral polyproteins (56). Although it has been reported which sequence motifs are responsible for localization of the HCV core protein to lipid droplets and nuclei, it is uncertain which sequences target the core protein to the ER and to mitochondria. In this study, we identified sequences related to localization of the mature core protein to the ER and to mitochondria.

Through heterologous expression of core-GFP fusion proteins containing a series of deletions, we determined that a sequence extending from amino acids 112 to 152 of the core protein is required for its localization at the mitochondrial outer membrane. Translocation of nucleus-encoded mitochondrial proteins is usually dependent on N-terminal sequences, referred to as mitochondrial targeting sequences (37). However, it is also true that a significant proportion of mitochondrial proteins lack these N-terminal mitochondrial targeting sequences. Specifically, a number of outer membrane proteins do not have cleavable sequences at their N termini; rather, they are targeted to mitochondria by means of internal or C-terminal signals (31).

Since it has been reported that amino acid sequences required for targeting to the outer mitochondrial membrane form a highly hydrophobic α-helical wheel, as seen in A-kinase associated protein 84/12 (4) and NADH-cytochrome *b* reduc-

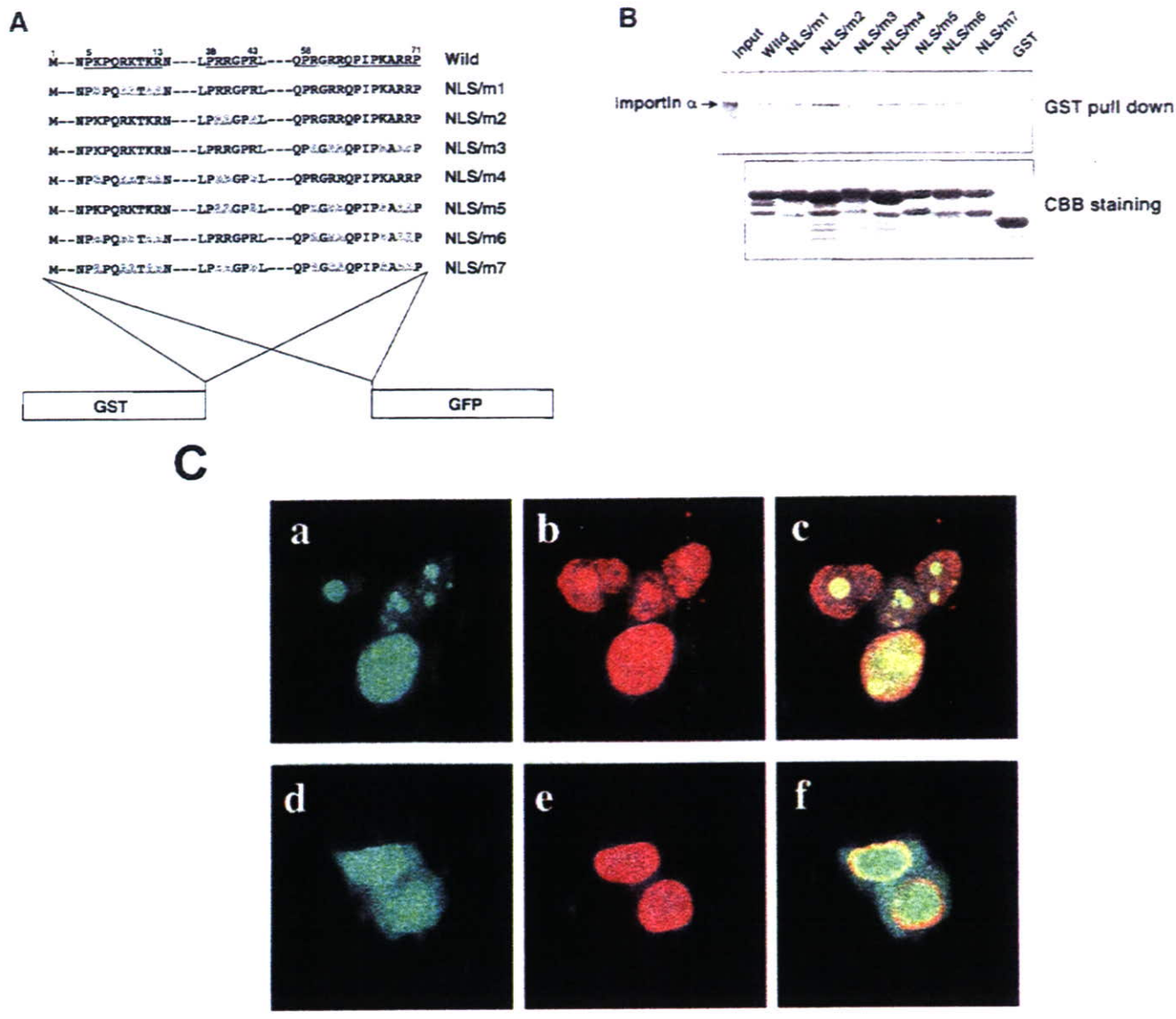


FIG. 7. Mutational analyses of NLS motifs in HCV core protein. (A) Schematic structures of fusion proteins and amino acid sequences corresponding to putative NLS motifs, three basic clusters (underlined) in the core protein. Two series of constructs fused with either GFP or GST were created. The mutated basic residues are indicated with outline letters. (B) GST pulldown assay. Equal amounts of GST fusions as described in A or GST alone was immobilized on glutathione-Sepharose 4B beads and incubated with in vitro-translated, [$^{35}$S]methionine-labeled importin-α. Bound material was separated by SDS-PAGE, and the amount of importin-α bound was detected by autoradiography. Direct electrophoretic separation of in vitro translation products served as a control (input). Coomassie brilliant blue staining of GST fusions and GST alone are shown in the bottom panel. (C) Confocal analysis of double staining for core-GFP fusion protein and HA-importin-α. 293T cells transfected with the wild-type core (1–71)-GFP (a to c) or NLS/m4 (d to f) expression plasmid and pCAG-HA-imp were allowed to express for 2 days. After the cells were fixed and permeabilized, they were incubated with a mouse anti-HA antibody. The red signals corresponding to HA-importin-α were obtained with a rhodamine-conjugated goat anti-mouse IgG secondary antibody (b and e). Overlay resulted in yellow signals indicative of colocalization (c and f). (D) Subcellular localization of GFP fusion proteins. GFP fusions with and without substitution mutations in the NLS motifs of the core protein as described in A were expressed in 293T cells. GFP images of the fixed cells were recorded.

tase (14), a predicted structure of an amphipathic α-helix present between amino acids 116 and 134 (Fig. 6B and C) possibly plays a role in directing the core protein to the mitochondrial outer membrane. Sequence comparisons demonstrate conservation of the amino acid sequence and secondary structure of the region, amino acids 112 to 152, among a variety of HCV isolates, including the infectious H77c clone (55), as well as a full-length adaptive replicon (3). To gain insight into the significance of the secondary structure of the region in targeting to the mitochondria, further structural and biochemical analyses are needed.

The association of HCV core protein with the mitochondrial membrane suggests that the core protein has the ability to modulate mitochondrial function, possibly by altering the permeability of the mitochondrial membrane. The core protein induces the production of cellular reactive oxygen species in

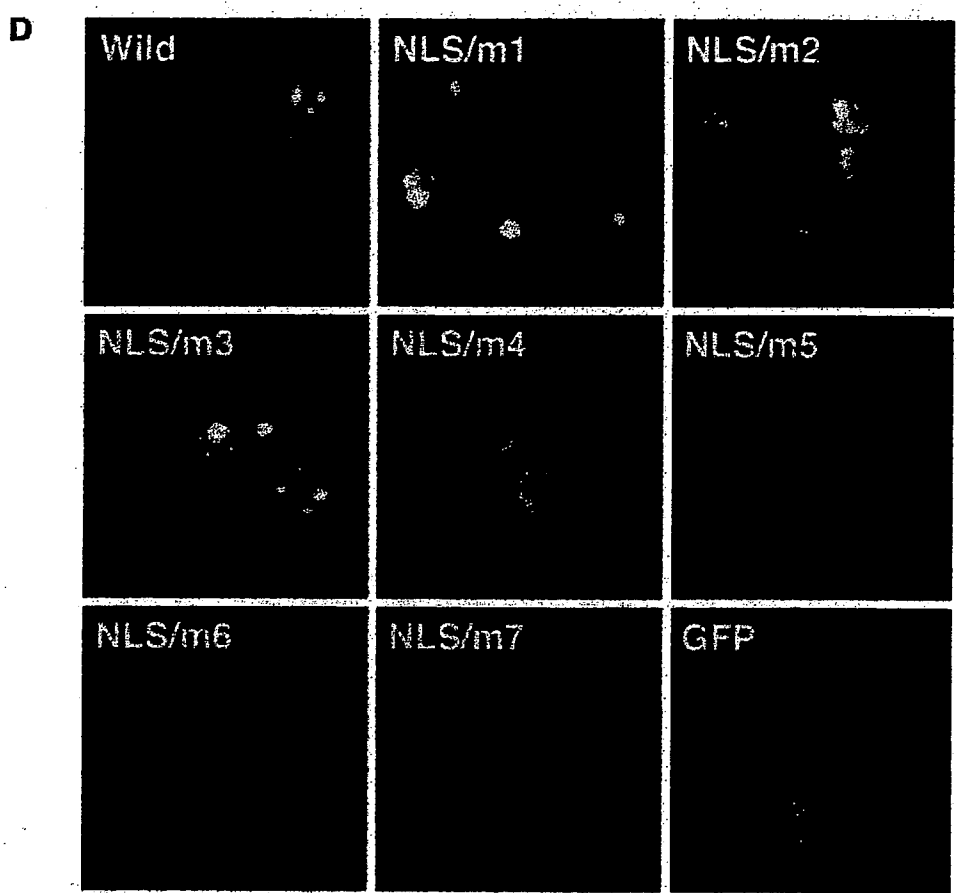


FIG. 7—*Continued.*

the livers of core-transgenic mice and in core-expressing cell lines (35). Reactive oxygen species, predominantly generated in mitochondria, induce genetic mutations and act as secondary messengers to regulate a variety of cellular functions, including gene expression and proliferation (1). Although the molecular mechanism by which core protein induces reactive oxygen species production is still unclear, HCV core protein is known to impair the mitochondrial electron transfer system (35). The core protein may also modulate apoptosis, since mitochondria play a major role in regulating programmed cell death. Expression of HCV proteins, including the core protein, suppresses the release of cytochrome *c* from mitochondria to the cytoplasm in HCV-transgenic mice, thus inhibiting Fas-mediated apoptosis (27).

Okamoto et al. recently reported that not only the C-terminal signal sequence but also amino acids 128 to 151 are required for ER retention of the core protein by using a series of N-terminally truncated core protein constructs (38). Here, in this study, we further showed that amino acids 112 to 152 mediate association of the core protein with the ER in the absence of the C-terminal signal sequence. Hope and McLauchlan demonstrated that the central domain of the core protein, amino acids 119 to 174, is important for association with lipid droplets (17). They also showed that this corresponding domain is shared with GB virus B, which is most closely related to HCV, but not with either pestiviruses or flaviviruses (18). It appears that the 41 residues identified as the sequence mediating association with the ER membrane in the present study are crucial for directing the core protein to lipid droplets, since the surface of lipid droplets must derive from the cytoplasmic side of the ER membrane.

The HCV core protein contains NLS sequences which are composed of three stretches of sequences rich in basic residues. These sequences were originally identified by experiments with fused forms of wild-type and mutated core proteins with β-galactosidase (6, 48). C-terminally truncated versions of the core protein localize exclusively to the nucleus (48). A fraction of the core protein is detected in the nucleus even when full-length HCV core gene is expressed (Fig. 2) and as described (34, 56). However, it is difficult to demonstrate clearly the nuclear localization of the core protein by immunofluorescence, presumably because of the instability of nuclearly localized core protein (49, 33). We only observed a nuclear staining pattern of the matured core protein after adding proteasome inhibitors to the culture (33).

Generally, NLS sequences fall into two categories; (i) monopartite NLSs, which contain a single cluster of basic residues, and (ii) bipartite NLSs, which contain two clusters of basic residues separated by an unconserved linker sequence of variable length (reviewed in reference 12). Nuclear translocation of an NLS-containing cargo protein is initiated when the soluble import receptor (importin) recognizes the NLS-contain-

ing protein within the cytoplasm. Importin-α contains an NLS-binding site(s), and importin-β docks importin-cargo complexes to the cytoplasmic filaments of a nuclear pore complex, after which translocation occurs through the nuclear pore. Thus, importin-α functions as an adaptor between the bona fide import receptor and the NLS-containing protein.

We further characterized the NLS of the core protein and found that each of the NLS motifs of the core protein is able to bind to importin-α and that at least two NLS motifs are required for efficient nuclear distribution of the core protein in cells. It appears that double mutations among three NLS motifs decrease the ability of the core protein to bind importin-α. These observations suggest that the binding of the double mutants with importin-α leads to no or little active translocation of the core protein into the nucleus. The double mutations may also block subsequent interactions with importin-β1, GTPase Ran, and/or NTF2/p10, which are required for translocation through the nuclear pore complexes.

The findings obtained in this study suggest that HCV core protein NLS motifs have a bipartite function. Crystallographic studies of monopartite (e.g., simian virus 40 large T antigen) and bipartite (e.g., nucleoplasmin) NLSs show that the basic residue clusters of bipartite NLSs occupy separate binding sites on importin-α. In contrast, while monopartite NLSs can bind to the same sites as bipartate NLSs on importin-α, they mainly bind to the N-terminal binding site, which is referred to as the major binding site on importin-α (9, 11). A recent report describes an importin-α variant with a mutation in the major site which results in decreased ability to bind both monopartite and bipartite NLSs. Another variant with a mutation in the minor site exhibits decreased binding only to bipartite NLS-containing proteins, making importin-α nonfunctional in vivo (22). Thus, we favor a model in which the core protein bipartite NLS, composed of any two of the three basic clusters, occupies both major and minor binding sites on importin-α, resulting in efficient nuclear translocation. Importin-α may be equally accessible to all clusters, given their close proximity to one another, as well as the distinct conformational flexibility of the ≈70-residue N-terminal region of the core protein.

With regard to the molecular mechanisms participating in nuclear localization of the core protein, Moriishi et al. found that PA28γ is involved in nuclear localization of the core protein. Interaction of the core protein with PA28γ plays an important role in retention of the core protein in the nucleus (33). Furthermore, in yeast cells, nuclear transport of the core protein requires the activity of the small GTPase Ran/Gsp1p and is mediated by Kap123p, but neither importin-α nor importin-β is involved (20). Differences in nucleocytoplasmic transport between yeast and mammalian cells might explain the inconsistencies observed in the present study. Further experiments are required to characterize the exact nature of the interaction between the core protein and components of the nuclear import machinery, particularly in cells where HCV is replicating.

In conclusion, the mature HCV core protein has an internal 41-amino-acid sequence mediating association of the viral protein with the ER and mitochondria. We also provide evidence for a novel class of bipartite NLS contained within the core protein, which comprises two of three basic motifs, thus enabling efficient nuclear targeting. Multiple functional domains influence the subcellular localization of the core protein, which ultimately depends on the balance of the respective signals.

## ACKNOWLEDGMENTS

We thank colleagues in the laboratories of the Department of Virology II at the National Institute of Infectious Diseases of Japan for providing advice and help. We especially thank Mami Matsuda and Makiko Yahata for assistance in sequencing and the preparation of experimental reagents and Tomoko Mizoguchi for secretarial work. We are grateful to Karsten Weis for providing us with the plasmid containing importin-α cDNA.

This work was supported in part by Second Term Comprehensive 10-Year Strategy for Cancer Control and Research on Emerging and Reemerging Infectious Diseases, Health Sciences Research Grants of the Ministry of Health, Labor and Welfare, and by the Program for Promotion of Fundamental Studies in Health Sciences of the Organization for Drug ADR Relief, R&D Promotion and Product Review of Japan (ID:01–3). This work was also supported in part by a Grant-in-Aid for Young Scientists from the Ministry of Education, Culture, Sports, Science and Technology to R.S. (15790244).

## REFERENCES

1. **Adler, V., Z. Yin, K. D. Tew, and Z. Ronai.** 1999. Role of redox potential and reactive oxygen species in stress signaling. Oncogene **18**:6104–6111.
2. **Barba, G., F. Harper, T. Harada, M. Kohara, S. Goulinet, Y. Matsuura, G. Eder, Z. Schaff, M. J. Chapman, T. Miyamura, and C. Bréchot.** 1997. Hepatitis C virus core protein shows a cytoplasmic localization and associates to cellular lipid storage droplets. Proc. Natl. Acad. Sci. USA **94**:1200–1205.
3. **Bukh, J., T. Pietschmann, V. Lohmann, N. Krieger, K. Faulk, R. E. Engle, S. Govindarajan, M. Shapiro, M. St Claire, and R. Bartenschlager.** 2002. Mutations that permit efficient replication of hepatitis C virus RNA in Huh-7 cells prevent productive replication in chimpanzees. Proc. Natl. Acad. Sci. USA **99**:14416–14421.
4. **Cardone, L., T. de Cristofaro, A. Affaitati, C. Garbi, M. D. Ginsberg, M. Saviano, S. Varrone, C. S. Rubin, M. E. Gottesman, E. V. Avvedimento, and A. Feliciello.** 2002. A-kinase anchor protein 84/121 are targeted to mitochondria and mitotic spindles by overlapping amino-terminal motifs. J. Mol. Biol. **320**:663–675.
5. **Chang, J., S. H. Yang, Y. G. Cho, S. B. Hwang, Y. S. Hahn, and Y. C. Sung.** 1998. Hepatitis C virus core from two different genotypes has an oncogenic potential but is not sufficient for transforming primary rat embryo fibroblasts in cooperation with the H-ras oncogene. J. Virol. **72**:3060–3065.
6. **Chang, S. C., J. H. Yen, H. Y. Kang, M. H. Jang, and M. F. Chang.** 1994. Nuclear localization signals in the core protein of hepatitis C virus. Biochem. Biophys. Res. Commun. **205**:1284–1290.
7. **Choo, Q. L., G. Kuo, A. J. Weiner, L. R. Overby, D. W. Bradley, and M. Houghton.** 1989. Isolation of a cDNA clone derived from a blood-borne non-A, non-B viral hepatitis genome. Science **244**:359–362.
8. **Choo, Q. L., K. H. Richman, J. H. Han, K. Berger, C. Lee, C. Dong, C. Gallegos, D. Coit, R. Medina-Selby, P. J. Barr, et al.** 1991. Genetic organization and diversity of the hepatitis C virus. Proc. Natl. Acad. Sci. USA **88**:2451–2455.
9. **Conti, E., M. Uy, L. Leighton, G. Blobel, and J. Kuriyan.** 1998. Crystallographic analysis of the recognition of a nuclear localization signal by the nuclear import factor karyopherin alpha. Cell **94**:193–204.
10. **Falcon, V., N. Acosta-Rivero, G. Chinea, M. C. de la Rosa, I. Menendez, S. Duenas-Carrera, B. Gra, A. Rodriguez, V. Tsutsumi, M. Shibayama, J. Luna-Munoz, M. M. Miranda-Sanchez, J. Morales-Grillo, and J. Kouri.** 2003. Nuclear localization of nucleocapsid-like particles and HCV core protein in hepatocytes of a chronically HCV-infected patient. Biochem. Biophys. Res. Commun. **310**:54–58.
11. **Fontes, M. R., T. Teh, and B. Kobe.** 2000. Structural basis of recognition of monopartite and bipartite nuclear localization sequences by mammalian importin-alpha. J. Mol. Biol. **297**:1183–1194.
12. **Görlich, D., and U. Kutay.** 1999. Transport between the cell nucleus and the cytoplasm. Annu. Rev. Cell. Dev. Biol. **15**:607–660.
13. **Grakoui, A., D. W. McCourt, C. Wychowski, S. M. Feinstone, and C. M. Rice.** 1993. Characterization of the hepatitis C virus-encoded serine proteinase: determination of proteinase-dependent polyprotein cleavage sites. J. Virol. **67**:2832–2843.
14. **Hahne, K., V. Haucke, L. Ramage, and G. Schatz.** 1994. Incomplete arrest in the outer membrane sorts NADH-cytochrome b5 reductase to two different submitochondrial compartments. Cell **79**:829–839.
15. **Harada, S., Y. Watanabe, K. Takeuchi, T. Suzuki, T. Katayama, Y. Takebe, I. Saito, and T. Miyamura.** 1991. Expression of processed core protein of hepatitis C virus in mammalian cells. J. Virol. **65**:3015–3021.
16. **Hijikata, M., N. Kato, Y. Ootsuyama, M. Nakagawa, and K. Shimotohno.** 1991. Gene mapping of the putative structural region of the hepatitis C virus

genome by in vitro processing analysis. Proc. Natl. Acad. Sci. USA 88:5547–5551.
17. **Hope, R. G., and J. McLauchlan.** 2000. Sequence motifs required for lipid droplet association and protein stability are unique to the hepatitis C virus core protein. J. Gen. Virol. 81:1913–1925.
18. **Hope, R. G., D. J. Murphy, and J. McLauchlan.** 2002. The domains required to direct core proteins of hepatitis C virus and GB virus-B to lipid droplets share common features with plant oleosin proteins. J. Biol. Chem. 277:4261–4270.
19. **Hüssy, P., H. Langen, J. Mous, and H. Jacobsen.** 1996. Hepatitis C virus core protein: carboxy-terminal boundaries of two processed species suggest cleavage by a signal peptide peptidase. Virology 224:93–104.
20. **Isoyama, T., S. Kuge, and A. Nomoto.** 2002. The core protein of hepatitis C virus is imported into the nucleus by transport receptor Kap123p but inhibits Kap121p-dependent nuclear import of yeast AP1-like transcription factor in yeast cells. J. Biol. Chem. 277:39634–39641.
21. **Lai, M. M., and C. F. Ware.** 2000. Hepatitis C virus core protein: possible roles in viral pathogenesis. Curr. Top. Microbiol. Immunol. 242:117–134.
22. **Leung, S. W., M. T. Harreman, M. R. Hodel, A. E. Hodel, and A. H. Corbett.** 2003. Dissection of the karyopherin alpha nuclear localization signal (NLS)-binding groove: functional requirements for NLS binding. J. Biol. Chem. 278:41947–41953.
23. **Liu, Q., C. Tackney, R. A. Bhat, A. M. Prince, and P. Zhang.** 1997. Regulated processing of hepatitis C virus core protein is linked to subcellular localization. J. Virol. 71:657–662.
24. **Lo, S. Y., F. Masiarz, S. B. Hwang, M. M. Lai, and J. H. Ou.** 1995. Differential subcellular localization of hepatitis C virus core gene products. Virology 213:455–461.
25. **Lo, S. Y., M. Selby, M. Tong, and J. H. Ou.** 1994. Comparative studies of the core gene products of two different hepatitis C virus isolates: two alternative forms determined by a single amino acid substitution. Virology 199:124–131.
26. **Lu, W., A. Strohecker, and J. H. Ou.** 2001. Post-translational modification of the hepatitis C virus core protein by tissue transglutaminase. J. Biol. Chem. 276:47993–47999.
27. **Machida, K., K. Tsukiyama-Kohara, E. Seike, S. Tone, F. Shibasaki, M. Shimizu, H. Takahashi, Y. Hayashi, N. Funata, C. Taya, H. Yonekawa, and M. Kohara.** 2001. Inhibition of cytochrome c release in Fas-mediated signaling pathway in transgenic mice induced to express hepatitis C viral proteins. J. Biol. Chem. 276:12140–12146.
28. **Matsumoto, M., S. B. Hwang, K. S. Jeng, N. Zhu, and M. M. Lai.** 1996. Homotypic interaction and multimerization of hepatitis C virus core protein. Virology 218:43–51.
29. **McLauchlan, J.** 2000. Properties of the hepatitis C virus core protein: a structural protein that modulates cellular processes. J. Viral Hepatitis 7:2–14.
30. **McLauchlan, J., M. K. Lemberg, G. Hope, and B. Martoglio.** 2002. Intramembrane proteolysis promotes trafficking of hepatitis C virus core protein to lipid droplets. EMBO J. 21:3980–3988.
31. **Mihara, K.** 2000. Targeting and insertion of nuclear-encoded preproteins into the mitochondrial outer membrane. Bioessays 22:364–371.
32. **Moradpour, D., C. Englert, T. Wakita, and J. R. Wands.** 1996. Characterization of cell lines allowing tightly regulated expression of hepatitis C virus core protein. Virology 222:51–63.
33. **Moriishi, K., T. Okabayashi, K. Nakai, K. Moriya, K. Koike, S. Murata, T. Chiba, K. Tanaka, R. Suzuki, T. Suzuki, T. Miyamura, and Y. Matsuura.** 2003. Proteasome activator PA28gamma-dependent nuclear retention and degradation of hepatitis C virus core protein. J. Virol. 77:10237–10249.
34. **Moriya, K., H. Fujie, Y. Shintani, H. Yotsuyanagi, T. Tsutsumi, K. Ishibashi, Y. Matsuura, S. Kimura, T. Miyamura, and K. Koike.** 1998. The core protein of hepatitis C virus induces hepatocellular carcinoma in transgenic mice. Nat. Med. 4:1065–1067.
35. **Moriya, K., K. Nakagawa, T. Santa, Y. Shintani, H. Fujie, H. Miyoshi, T. Tsutsumi, T. Miyazawa, K. Ishibashi, T. Horie, K. Imai, T. Todoroki, S. Kimura, and K. Koike.** 2001. Oxidative stress in the absence of inflammation in a mouse model for hepatitis C virus-associated hepatocarcinogenesis. Cancer Res. 61:4365–4370.
36. **Moriya, K., H. Yotsuyanagi, Y. Shintani, H. Fujie, K. Ishibashi, Y. Matsuura, T. Miyamura, and K. Koike.** 1997. Hepatitis C virus core protein induces hepatic steatosis in transgenic mice. J. Gen. Virol. 78:1527–1531.
37. **Neupert, W.** 1997. Protein import into mitochondria. Annu. Rev. Biochem. 66:863–917.
38. **Okamoto, K., K. Moriishi, T. Miyamura, and Y. Matsuura.** 2004. Intramembrane proteolysis and endoplasmic reticulum retention of hepatitis C virus core protein. J. Virol. 78:6370–6380.
39. **Okuda, M., K. Li, M. R. Beard, L. A. Showalter, F. Scholle, S. M. Lemon, and S. A. Weinman.** 2002. Mitochondrial injury, oxidative stress, and antioxidant gene expression are induced by hepatitis C virus core protein. Gastroenterology 122:366–375.
40. **Perlemuter, G., A. Sabile, P. Letteron, G. Vona, A. Topilco, Y. Chretien, K. Koike, D. Pessayre, J. Chapman, G. Barba, and C. Bréchot.** 2002. Hepatitis C virus core protein inhibits microsomal triglyceride transfer protein activity and very low density lipoprotein secretion: a model of viral-related steatosis. FASEB J. 16:185–194.
41. **Ralston, R., K. Thudium, K. Berger, C. Kuo, B. Gervase, J. Hall, M. Selby, G. Kuo, M. Houghton, and Q. L. Choo.** 1993. Characterization of hepatitis C virus envelope glycoprotein complexes expressed by recombinant vaccinia viruses. J. Virol. 67:6753–6761.
42. **Ray, R. B., L. M. Lagging, K. Meyer, and R. Ray.** 1996. Hepatitis C virus core protein cooperates with ras and transforms primary rat embryo fibroblasts to tumorigenic phenotype. J. Virol. 70:4438–4443.
43. **Roth, J., D. J. Taatjes, and M. J. Warhol.** 1989. Prevention of non-specific interactions of gold-labeled reagents on tissue sections. Histochemistry 92: 47–56.
44. **Sabile, A., G. Perlemuter, F. Bono, K. Kohara, F. Demaugre, M. Kohara, Y. Matsuura, T. Miyamura, C. Brechot, and G. Barba.** 1999. Hepatitis C virus core protein binds to apolipoprotein AII and its secretion is modulated by fibrates. Hepatology 30:1064–1076.
45. **Santolini, E., G. Migliaccio, and N. La Monica.** 1994. Biosynthesis and biochemical properties of the hepatitis C virus core protein. J. Virol. 68: 3631–3641.
46. **Selby, M. J., Q. L. Choo, K. Berger, G. Kuo, E. Glazer, M. Eckart, C. Lee, D. Chien, C. Kuo, and M. Houghton.** 1993. Expression, identification and subcellular localization of the proteins encoded by the hepatitis C viral genome. J. Gen. Virol. 74:1103–1113.
47. **Shimoike, T., S. Mimori, H. Tani, Y. Matsuura, and T. Miyamura.** 1999. Interaction of hepatitis C virus core protein with viral sense RNA and suppression of its translation. J. Virol. 73:9718–9725.
48. **Suzuki, R., Y. Matsuura, T. Suzuki, A. Ando, J. Chiba, S. Harada, I. Saito, and T. Miyamura.** 1995. Nuclear localization of the truncated hepatitis C virus core protein with its hydrophobic C terminus deleted. J. Gen. Virol. 76:53–61.
49. **Suzuki, R., K. Tamura, J. Li, K. Ishii, Y. Matsuura, T. Miyamura, and T. Suzuki.** 2001. Ubiquitin-mediated degradation of hepatitis C virus core protein is regulated by processing at its carboxyl terminus. Virology 280:301–309.
50. **Tanaka, Y., T. Shimoike, K. Ishii, R. Suzuki, T. Suzuki, H. Ushijima, Y. Matsuura, and T. Miyamura.** 2000. Selective binding of hepatitis C virus core protein to synthetic oligonucleotides corresponding to the 5′ untranslated region of the viral genome. Virology 270:229–236.
51. **Tellinghuisen, T. L., and C. M. Rice.** 2002. Interaction between hepatitis C virus proteins and host cell factors. Curr. Opin. Microbiol. 5:419–427.
52. **Thomson, M., and T. J. Liang.** 2000. Molecular biology of hepatitis C virus, p. 1–23. *In* T. J. Liang and J. H. Hoofnagle (ed.), Hepatitis C. Academic Press, San Diego, Calif.
53. **Weihofen, A., K. Binns, M. K. Lemberg, K. Ashman, and B. Martoglio.** 2002. Identification of signal peptide peptidase, a presenilin-type aspartic protease. Science 296:2215–2218.
54. **Weis, K., I. W. Mattaj, and A. I. Lamond.** 1995. Identification of hSRP1 alpha as a functional receptor for nuclear localization sequences. Science 268:1049–1053.
55. **Yanagi, M., R. H. Purcell, S. U. Emerson, and J. Bukh.** 1997. Transcripts from a single full-length cDNA clone of hepatitis C virus are infectious when directly transfected into the liver of a chimpanzee. Proc. Natl. Acad. Sci. USA 94:8738–8743.
56. **Yasui, K., T. Wakita, K. Tsukiyama-Kohara, S. I. Funahashi, M. Ichikawa, T. Kajita, D. Moradpour, J. R. Wands, and M. Kohara.** 1998. The native form and maturation process of hepatitis C virus core protein. J. Virol. 72:6048–6055.

厚生労働科学研究費補助金
肝炎等克服緊急対策研究事業

# C型肝炎新規治療開発に資するプロテオーム解析を用いた治療標的分子の網羅的検索系とヒト肝細胞キメラマウスHCV感染モデルを用いた実証系の開発に関する研究

研究成果（平成18年度ー19年度）

主任研究者　茶山　一彰

平成20年（2008）年3月

# 研究成果—平成 18 年度

*Journal of General Virology* (2007), 88, 432–440 DOI 10.1099/vir.0.82319-0

# Dual effect of APOBEC3G on *Hepatitis B virus*

Chiemi Noguchi,[1,2] Nobuhiko Hiraga,[1,2] Nami Mori,[1,2] Masataka Tsuge,[1,2] Michio Imamura,[1,2] Shoichi Takahashi,[1,2] Yoshifumi Fujimoto,[2,3] Hidenori Ochi,[2,3] Hiromi Abe,[1,3] Toshiro Maekawa,[3] Hiromi Yatsuji,[1,4] Kotaro Shirakawa,[5] Akifumi Takaori-Kondo[5] and Kazuaki Chayama[1,2,3]

[1]Department of Medicine and Molecular Science, Division of Frontier Medical Science, Programs for Biomedical Research, Graduate School of Biomedical Sciences, Hiroshima University, 1-2-3 Kasumi, Minami-ku, Hiroshima-shi 734-8551, Japan

[2]Liver Research Project Center, Hiroshima University, Hiroshima, Japan

[3]Laboratory for Liver Diseases, SNP Research Center, The Institute of Physical and Chemical Research (RIKEN), Yokohama 230-0045, Japan

[4]Department of Gastroenterology, Toranomon Hospital, Tokyo, Japan

[5]Department of Hematology and Oncology, Graduate School of Medicine, Kyoto University, Kyoto 606-8507, Japan

Correspondence
Kazuaki Chayama
chayama@hiroshima-u.ac.jp

Received 22 June 2006
Accepted 10 October 2006

G to A hypermutation of *Hepatitis B virus* (HBV) and retroviruses appears as a result of deamination activities of host APOBEC proteins and is thought to play a role in innate antiviral immunity. Alpha and gamma interferons (IFN-$\alpha$ and -$\gamma$) have been reported to upregulate the transcription of APOBEC3G, which is known to reduce the replication of HBV. We investigated the number of hypermutated genomes under various conditions by developing a quantitative measurement. The level of hypermutated HBV in a HepG2 cell line, which is semi-permissive for retrovirus, was 2.3 in $10^4$ HBV genomes, but only 0.5 in $10^4$ in permissive Huh7 cells. The level of APOBEC3G mRNA was about ten times greater in HepG2 cells than in Huh7 cells. Treatment of HepG2 cells with either IFN-$\alpha$ or -$\gamma$ increased the transcription of APOBEC3G and hypermutation of HBV. These mRNAs and hypermutation of HBV genomes were induced more prominently by IFN-$\gamma$ than by IFN-$\alpha$. Both IFNs decreased the number of replicative intermediate of HBV. Overexpression of APOBEC3G reduced the number of replicative intermediate of HBV and increased hypermutated genomes 334 times, reaching 968 in $10^4$ genomes. Deamination-inactive APOBEC3G did not induce hypermutation, but reduced the virus equally. Our results suggest that APOBEC3G, upregulated by IFNs, has a dual effect on HBV: induction of hypermutation and reduction of virus synthesis. The effect of hypermutation on infectivity should be investigated further.

## INTRODUCTION

*Hepatitis B virus* (HBV) is a small, enveloped DNA virus with partially double-stranded DNA as a genome (Ganem & Schneider, 2001; Seeger & Mason, 2000). The virus replicates through transcription of pregenome RNA and reverse transcription, like retroviruses (Skalka & Goff, 1993; Summers & Mason, 1982). Infection with HBV causes chronic hepatitis and often leads to liver cirrhosis and hepatocellular carcinoma (Wright & Lau, 1993; Bruix & Llovet, 2003; Ganem & Prince, 2004).

Recent reports have shown that a cytidine deaminase, APOBEC3G, which is packaged in human immunodeficiency virus (HIV) virions in non-permissive cells, induces G to A hypermutation to a nascent reverse transcript of HIV and serves as part of the innate antiviral activity (Mangeat *et al.*, 2003; Zhang *et al.*, 2003; Lecossier *et al.*, 2003; Harris *et al.*, 2003). Recent studies have demonstrated that a small number of HBV DNA in serum samples of patients with chronic HBV infection contains hypermutated genomes (Gunther *et al.*, 1997; Suspene *et al.*, 2005a; Noguchi *et al.*, 2005). We reported previously that there are small numbers of hypermutated genomes in serum samples of the majority of patients with chronic HBV infection and that G to A hypermutation could be induced in cultured liver cells derived from HepG2 cell lines (Noguchi *et al.*, 2005) using a peptide nucleic acid-mediated PCR clamping method. Suspene *et al.* (2005a) developed the more sensitive differential DNA denaturation (3D)-PCR method to detect hypermutated genomes and found that some APOBEC proteins induce G to A, and in some cases C to T, hypermutations in HBV DNA (Suspene *et al.*, 2005a). Why only a very small proportion of the HBV genome is hypermutated is unknown at present. Furthermore, the

 

mechanism that controls the level of APOBEC protein expression and degree of hypermutation has not been fully investigated. Recently, Tanaka *et al.* (2006) identified an interferon (IFN)-stimulated response element (ISRE) in the promoter region of APOBEC3G and showed that IFN-α upregulates transcription of APOBEC3G. Peng *et al.* (2006) also reported that IFN-α and -γ upregulate mRNA transcription of APOBEC proteins. However, these reports did not analyse whether increased numbers of APOBEC proteins actually increase hypermutation. More recently, Bonvin *et al.* (2006) demonstrated that IFN induces transcription of APOBEC proteins and increases hypermutation of HBV.

IFNs are cytokines that play a major role against many pathogens (Samuel, 2001; Colonna *et al.*, 2002; Grandvaux *et al.*, 2002). We also reported in a previous study that both IFN-α and -γ reduce virus replication in stably HBV-transfected cell lines without inducing a remarkable increase in G to A hypermutation (Noguchi *et al.*, 2005). However, the method used in previous experiments for detection of hypermutation was not as sensitive as the method of Suspene *et al.* (2005a, b) and not quantitative. To assess the level of hypermutation, a reliable measurement of hypermutated genome is needed. In the present study, we developed a new and sensitive method for the measurement of hypermutated genome levels. Using this method, we show here that both IFN-α and -γ increased the levels of hypermutated genomes in cultured cell lines. Furthermore, both IFNs increased the mRNA level of APOBEC3G. We also performed overexpression experiments to examine whether APOBEC3G and its inactive mutants increase the levels of hypermutation and reduce HBV replication.

## METHODS

**Plasmid constructs.** The expression vector for haemagglutinin (HA)-tagged human APOBEC3G, pcDNA3/HA-A3G, was constructed as described previously (Kobayashi *et al.*, 2004). APOBEC3F cDNA was obtained by modifying APOBEC3F like (IMAGE clones from Open Biosystems) to have the same sequence as human APOBEC3F transcript variant 1 (GenBank NM_145298) and cloned into pcDNA3/HA (Invitrogen). APOBEC3G mutants were constructed using a QuikChange mutagenesis kit (Stratagene). The construction of wild-type HBV 1.4 genome length, pTRE-HB-wt, has been described previously (GenBank accession no. AB206816) (Tsuge *et al.*, 2005).

**Cell culture and transfection.** Huh7 and HepG2 cell lines were grown in Dulbecco's modified Eagle's medium supplemented with 10 % (v/v) fetal calf serum at 37 °C in 5 % $CO_2$. Cells were seeded to semi-confluence in six-well tissue culture plates. Transient transfection of the plasmids into HepG2 and Huh7 cell lines was performed using *Trans*IT-LT1 (Mirus) according to the instructions provided by the supplier. A plasmid encoding a secreted form of human placental alkaline phosphatase (SEAP) was co-transfected to adjust the transfection efficiency. The SEAP assay in the culture medium was performed using the Great EscAPe SEAP Reporter System 3 (BD Bioscience).

T23 cells are HepG2 cells stably transfected with the plasmid pTRE-HB-wt. They were cultured using a method described previously (Tsuge *et al.*, 2005). Cells were seeded to semi-confluence in six-well tissue culture plates and then treated with medium containing either IFN-α (Hayashibara Biochemical Laboratories) or IFN-γ (Shionogi & Co.). The cells were harvested 12–72 h after IFN treatment. Core-associated HBV DNA was extracted from the cells for HBV DNA quantification and quantitative analysis of G to A hypermutated genomes (Noguchi *et al.*, 2005).

**Analysis of core-associated HBV DNA.** The cells were harvested 4 days after transfection and lysed with 250 µl lysis buffer [10 mM Tris/HCl pH 7.4, 140 mM NaCl and 0.5 % (v/v) NP-40] followed by centrifugation for 2 min at 15 000 *g*. The core-associated HBV genome was immunoprecipitated from the supernatant by mouse anti-core monoclonal antibody anti-HBc determinant α (Institute of Immunology, Tokyo, Japan) and subjected to quantitative analysis after SDS/proteinase K digestion followed by phenol extraction and ethanol precipitation. Quantitative analysis was performed by real-time PCR using the 7300 Real-Time PCR system (Applied Biosystems). The primers used for amplification were #1, 5′-ACTTCAACCCCAACAMRRATCA-3′ (nt 2978–2999) [numbers are those of HBV subtype C reported by Norder *et al.* (1994)] and #2, 5′-AGAGYTTGKTGGAATGTKGTGGA-3′ (nt 24–1), where M is A/C, R is G/A, Y is T/C and K is G/T. The probe was a 6-carboxyfluorescein (FAM)-labelled minor-groove binder (MGB) probe, 5′-(FAM)-TTAGAGGTGGAGAGATGG-(MGB)-3′ (nt 3184–3167). Real-time PCRs were set up in 25 µl TaqMan Universal Master Mix with 1 µl DNA solution, 0.9 µM each primer and 0.25 µM probe. The amplification conditions were 2 min at 50 °C, 10 min at 95 °C, followed by 40 cycles of amplification (denaturation at 95 °C for 15 s, annealing at 55 °C for 30 s and extension at 62 °C for 90 s).

**Amplification and analysis of hypermutated HBV genomes by 3D-PCR.** HBV DNA was extracted from 100 µl serum obtained from a chronic HBV carrier (genotype C) by SMITEST (MBL International) and was dissolved in 20 µl $H_2O$. Hypermutated genomes were detected by modified 3D-PCR using primers #1 and #2 and DNA solution from serum containing $8.0 \times 10^7$ or $2.3 \times 10^5$ copies of core-associated HBV DNA in 25 µl of 100 mM Tris/HCl pH 8.3, 50 mM KCl, 15 mM $MgCl_2$, 0.2 mM each dNTP, 10 pmol each primer and 1.25 U *Taq* DNA polymerase (Gene Taq, Nippon Gene Co.), together with 0.25 µg anti-*Taq* high (TOYOBO Co.). The amplification conditions included an initial denaturation step at 83–95 °C for 5 min, followed by 45 cycles of denaturation at 83–95 °C for 1 min, annealing at 50 °C for 30 s, extension at 72 °C for 30 s followed by 10 min of final extension. Amplicons were separated by electrophoresis on 2 % (w/v) agarose gel, cloned and sequenced in an ABI PRISM 3130 Genetic Analyzer with a BigDye Terminator version 3.1 cycle sequencing ready reaction kit (Applied Biosystems). The PCR products were also analysed on Hanse Analytik (HA)-yellow gel as described previously (Suspene *et al.*, 2005b; Tsuge *et al.*, 2005; Abu-Daya *et al.*, 1995).

**Quantitative analysis of hypermutated genomes by real-time PCR.** Hypermutated genomes were quantified by real-time PCR using the 7300 Real-Time PCR system (Applied Biosystems) and the above primers and probes. The amplification conditions included activation at 95 °C for 10 min followed by initial denaturation at 88 °C for 20 min and 45 cycles of amplification (denaturation at 88 °C for 15 s, annealing at 50 °C for 30 s and extension at 62 °C for 90 s). We chose 88 °C as this temperature is appropriate for detection of about 20 % hypermutated genomes. There are 200–300 such hypermutated genomes in $10^4$ genomes present in HepG2 cells transiently transfected with APOBEC3G. The buffer comprised 10 mM Tris/HCl pH 8.3, 50 mM KCl, 3 mM $MgCl_2$, 10 mM EDTA, 60 nM Passive Reference 1 (Applied Biosystems), 0.2 mM each dNTP, 0.9 µM each primer, 0.25 µM probe, $5 \times 10^6$ copies of HBV DNA

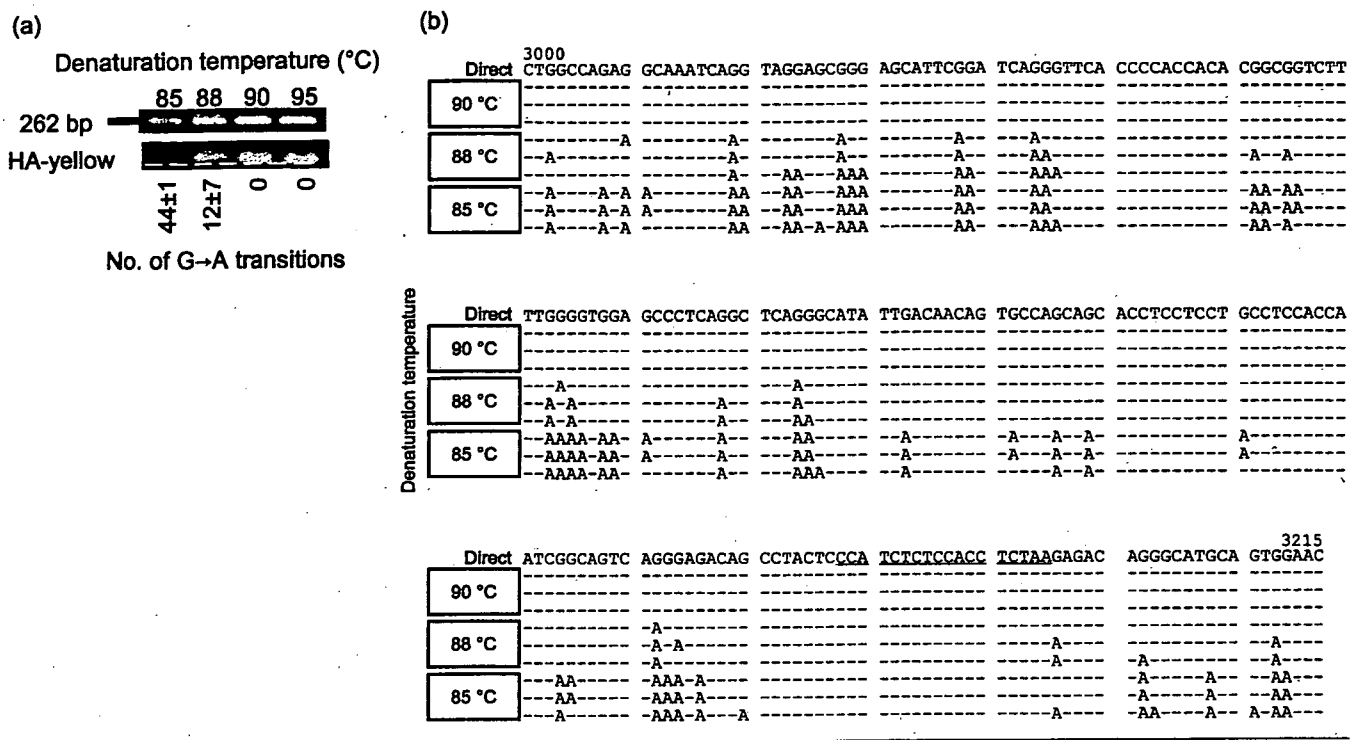


**Fig. 1.** Amplification of HBV DNA by 3D-PCR. (a) Detection of hypermutated genomes by HA-yellow agarose gel electrophoresis. The numbers of G to A transitions are expressed as means ± SD generated from the sequence analysis of five independent clones from PCR products. The white dotted line was added to help visualize the retardation of AT-rich DNA in HA-yellow agarose gel. (b) Nucleotide sequences of HBV amplified by 3D-PCR. The nucleotide sequences obtained by direct sequencing are used as a reference sequence. The nucleotide sequences where the probe hybridizes are underlined. Note that the number of G to A mutations correlates with denaturation temperature.

and 0.625 U AmpliTaq Gold DNA polymerase (Applied Biosystems) in a final volume of 25 µl. A standard curve was constructed by the simultaneous amplification of serial dilutions of the 3D-PCR products.

**Western blot analysis.** Cell lysates were prepared as described above, resolved on 10 % (w/v) SDS-polyacrylamide gels and transferred to nitrocellulose membranes (Whatman) via electro-blotting. The membranes were incubated with anti-haemagglutinin fusion epitope monoclonal antibody (Roche) or with anti-$\beta$-actin monoclonal antibody (Sigma-Aldrich) followed by incubation with horseradish peroxidase-conjugated donkey anti-rabbit antibody or sheep anti-mouse immunoglobulin (Amersham Biosciences). Proteins were visualized via the ECL system (Amersham Biosciences).

**Quantification of mRNA of APOBEC3G or APOBEC3F by reverse transcription and real-time PCR.** Total RNA was extracted from HepG2 cell lines by using an RNeasy Mini kit (Qiagen). The RNA was reverse transcribed with random primers and Moloney murine leukemia virus reverse transcriptase (ReverTra Ace, TOYOBO Co.) at 42 °C for 60 min according to the instructions provided by the manufacturer. Quantitative analysis of APOBEC3G and APOBEC3F cDNA was performed by real-time PCR using TaqMan Gene Expression assays (Applied Biosystems). To confirm that the APOBEC3G and -3F PCR primers specifically amplify the target genes, quantitative PCR on the expression plasmids encoding human APOBEC3G and -3F, used as templates, was performed. No cross amplification was observed, even when we used $10^7$ copies of APOBEC3G plasmid in the amplification reaction of APOBEC3F and vice versa. A standard curve was constructed by the amplification of serial dilutions of the known number of plasmids containing human APOBEC3G and APOBEC3F. The target cDNA was normalized to the endogenous RNA level of the housekeeping reference gene glyceraldehyde-3-phosphate dehydrogenase (GAPDH). The primers and FAM-labelled probe used to quantify GAPDH were purchased from Applied Biosystems.

**Infectivity of luciferase reporter viruses produced from HepG2 and Huh7 cell lines.** Luciferase reporter viruses with or without viral infectivity factor (Vif) were prepared by co-transfection of pNL43/ΔEnv-Luc (wild-type) or pNL43/ΔEnvΔvif-Luc (ΔVif) plus pVSV-G together with a mock vector or expression vectors for A3G by Lipofectamine (Invitrogen) as described previously (Janini *et al.*, 2001; Shindo *et al.*, 2003). Productive infection was measured by luciferase activity. Values were presented as percentage of infectivity relative to the value of each virus without expression of APOBEC3G proteins.

## RESULTS

### Quantitative analysis of hypermutated genome by real-time PCR

Using serum samples from a patient with a high viral load, we amplified a large number of hypermutated genomes by 3D-PCR and detected them by HA-yellow agarose gel electrophoresis (Fig. 1a). Nucleotide sequence analysis

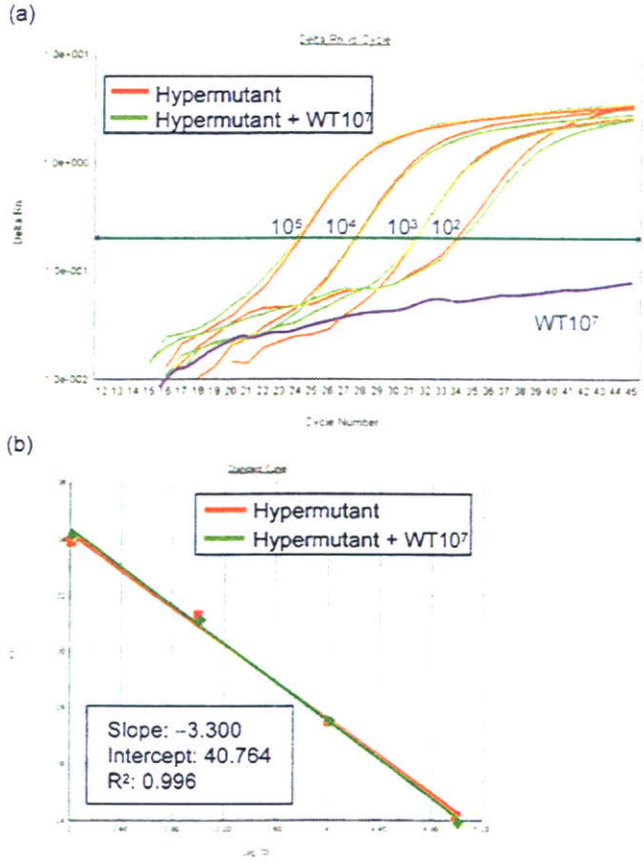


**Fig. 2.** Quantitative measurement of hypermutated HBV DNA using 3D-PCR combined with real-time PCR. The indicated numbers ($10^2$–$10^5$) of hypermutated genomes alone (orange lines) and a mixture of wild-type plus hypermutated genomes (green lines) were amplified by 3D-PCR. 3D-PCR did not result in amplification of wild-type sequence (purple line). Denaturation temperature was 88 °C.

showed detection of more heavily hypermutated genomes at lower denaturation temperatures (Fig. 1b). To develop quantitative measurement, we selected sequences with many G residues, designed primers that contained only a small number of G residues and used degenerate primers. A probe sequence was designed without a G residue. Using this primer and probe set, we could amplify only hypermutated genomes (Fig. 2). When hypermutated and non-mutated genomes were co-amplified, only hypermutated genomes were successfully amplified using the above primer and probe set (Fig. 2b). Non-hypermutated genomes ($10^7$ copies) were not amplified, although conventional PCR amplified both mutated and non-mutated genomes equally (data not shown). We also tried to detect only slightly (four of the 58 G residues) mutated genomes by 3D-PCR, but could not detect such genomes. It should thus be noted that the quantitative measurement we developed in this study detects only hypermutated genomes.

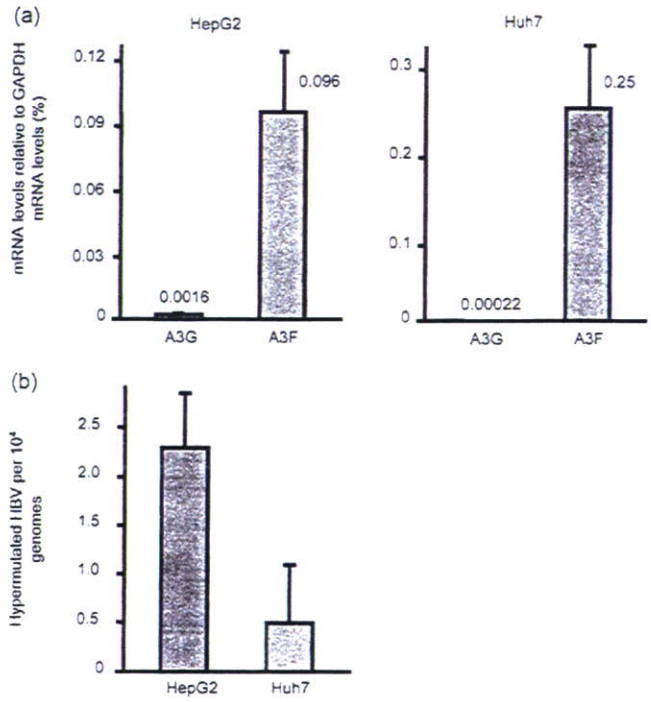


**Fig. 3.** Expression levels of APOBEC3G and -3F protein mRNAs in HepG2 and Huh7 cell lines. (a) mRNAs were extracted from cultured cell lines and the number of mRNA was quantified by real-time PCR with a probe for APOBEC3G and -3F. The expression levels were expressed as a percentage of GAPDH mRNA. (b) Number of hypermutated HBV genomes measured by real-time 3D-PCR in HepG2 and Huh7 cell lines transiently transfected with pTRE-HBV-wt. Results are means ± SD values of three independent experiments.

## Detection of APOBEC3G mRNA and hypermutated genomes in semi-permissive and permissive cell lines

In retrovirus studies, it is known that some cell lines allow production of infectious retrovirus virions with Vif deficiency (permissive cells) while others do not. The difference between semi-permissive and permissive cell lines is the expression of APOBEC3G (Mangeat *et al.*, 2003; Zhang *et al.*, 2003; Lecossier *et al.*, 2003; Harris *et al.*, 2003; Shirakawa *et al.*, 2006). Thus, we examined the expression of APOBEC3G in both HepG2 and Huh7 cell lines. The APOBEC3G mRNA level detected by real-time PCR was very low (approx. 0.002 % relative to GAPDH mRNA) and about ten times greater in HepG2 cells than in Huh7 cells (Fig. 3a).

The number of hypermutated genomes in HepG2 cells transiently transfected with pTRE-HB-wt was about five times that in Huh7 cells (Fig. 3b). Vif-deficient HIV-1 virions produced from HepG2 cell exhibited very low infectivity compared with wild-type (Fig. 4a). In contrast, the infectivity of HIV-1 virions produced by Huh7 was

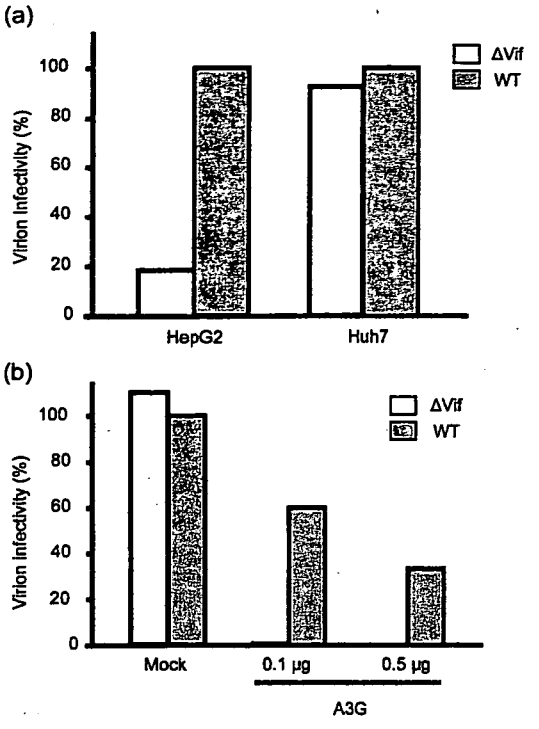


**Fig. 4.** Infectivity of HIV-1 virions produced from HepG2 and Huh7 cell lines. (a) Wild-type and mutant viruses lacking Vif protein produced from the two cell lines were examined for infectivity as described in Methods. The relative infectivity of the wild-type is shown. (b) Effect of APOBEC3G (A3G) expression on infectivity. HIV-1 virions produced by Huh7 cells co-transfected with the indicated number of APOBEC3G expression plasmid were used for measurement of infectivity.

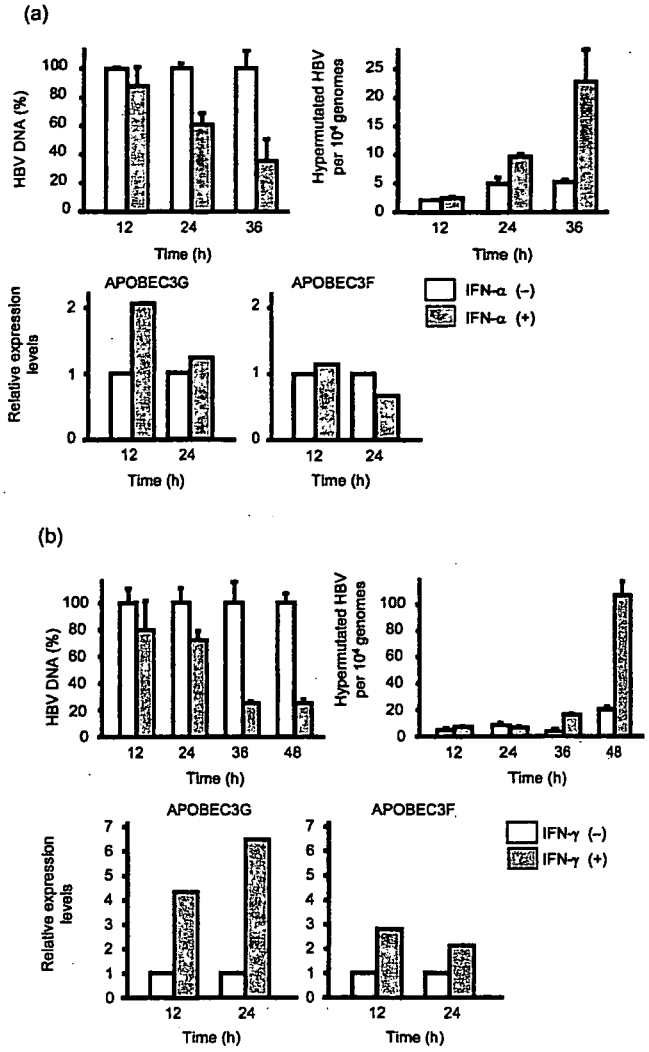


**Fig. 5.** Effects of IFN-α and -γ on HBV-producing cells. (a) The IFN-α-treated and -untreated HBV-producing T23 cell line was harvested at the indicated time after IFN treatment and examined for the number of core-associated HBV DNA, the number of hypermutated genome and mRNAs of APOBEC3G and APOBEC3F. (b) IFN-γ-treated and -untreated HBV-producing T23 cell line was examined as described in (a). Results are means ± SD values of three independent experiments.

similar to that of the wild-type virus (Fig. 4a). Transient expression experiments showed that the expression of APOBEC3G in Huh7 cell lines reduced infectivity of wild-type HIV-1 produced in these cell lines in a dose-dependent manner (Fig. 4b). Infectivity of Vif-deficient HIV-1 was reduced to almost undetectable levels (Fig. 4b). Thus, APOBEC3G effectively suppressed the production of infectious HIV in these cell lines.

## Both IFN-α and -γ induce APOBEC3G mRNA expression and hypermutation of HBV genomes and reduce replication of HBV

We treated HepG2 cell lines stably transfected with 1.4 genome length construct HBV (Tsuge *et al.*, 2005) with either IFN-α or -γ to examine their influence on the expression of APOBEC3G mRNA and G to A hypermutation of HBV genomes. Chronological studies showed that the core-associated HBV DNA in the stably HBV-producing cell line gradually decreased until 36 h after IFN-α treatment (Fig. 5a). Expression levels of APOBEC3G mRNA, but not those of APOBEC3F, increased in this cell line at 12 h after the IFN treatment (Fig. 5a). Hypermutated genomes in this cell line increased with time until 36 h after IFN-α treatment. Similarly, the core-associated HBV DNA decreased gradually to about 20 % of the levels in untreated cells after IFN-γ treatment (Fig. 5b). The increase in APOBEC3G mRNA expression was more prominent after IFN-γ than after IFN-α treatment. The level of APOBEC3F mRNA was also about double that of untreated cells. G to A hypermutation of HBV genomes increased markedly with time after IFN-γ treatment (Fig. 5b).

We further examined the effect of IFN on reduction of HBV replication and induction of hypermutation by comparing the effects of different doses of IFN-α and -γ. Both IFN-α

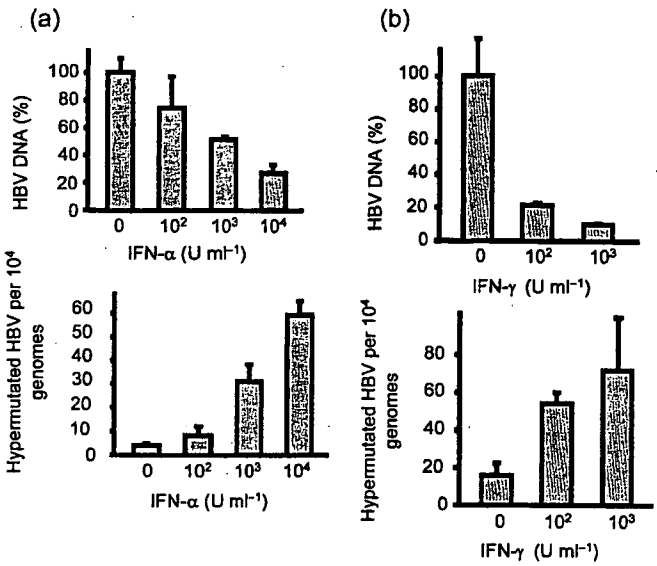


**Fig. 6.** Dose-dependent reduction of HBV replication and hypermutation of genomic sequences. HBV-producing cell line T23 was harvested after (a) IFN-$\alpha$ and (b) IFN-$\gamma$ treatment for 72 h. The number of core-associated HBV DNA and the number of hypermutated genomes were measured. Results are means ± SD values of three independent experiments.

and -$\gamma$ treatment decreased core-associated HBV DNA in a dose-dependent manner (Fig. 6). Hypermutation of HBV genomes also increased with higher doses of IFN (Fig. 6).

## Expression of APOBEC3G increases hypermutation of the HBV genome

To confirm that the increase in hypermutation of the HBV genome is induced by the effect of APOBEC3G, we performed expression experiments of APOBEC3G and its deaminase function-deficient mutants into HepG2 cell lines and measured the number of hypermutated HBV genomes. Transient expression experiments showed that the number of HBV DNA was decreased by co-transfection of APOBEC3G in HepG2 cells (Fig. 7a). 3D-PCR and detection with HA-yellow agarose gel electrophoresis showed the presence of heavily hypermutated genomes (Fig. 7b). No amplification was observed at the 81 °C denaturation temperature (data not shown). Quantitative analysis showed an about 334-fold increase in hypermutated genomes compared with mock-transfected control cells (Fig. 7c). However, the proportion of hypermutated genomes was 9.68 % (968 in $10^4$ genomes).

To confirm the effect of APOBEC3G on HBV hypermutation, we transfected wild-type and inactive mutants of APOBEC3G (Fig. 8a, b) into Huh7 cells. Wild-type APOBEC3G effectively induced hypermutation of HBV genomes and reduced the replication of HBV. In contrast, insufficient deaminase activity in the E67Q mutant induced less hypermutation of HBV genomes than in the wild-type. No increase in hypermutation was observed in cell lines transfected with deamination-defective E259Q and E67Q/E259Q mutants, although the number of HBV replication was reduced in these cells (Fig. 8a). We observed similar reduction in HBV replication by transient transfection of APOBEC3F. Induction of hypermutation by APOBEC3F was less efficient than by wild-type and the E67Q mutant of

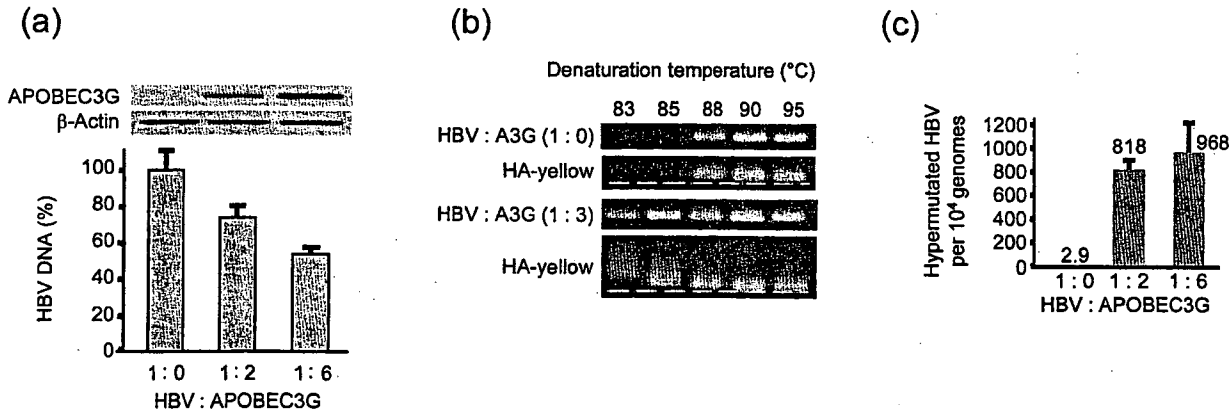


**Fig. 7.** Effects of APOBEC3G expression on HBV hypermutation. A plasmid containing 1.4 genome length HBV DNA was co-transfected with pcDNA3/HA-A3G into HepG2 cells. At 72 h after transfection, the cells were harvested. (a) Quantification of core-associated HBV DNA and Western blot analysis of cytoplasmic extracts with anti-HA or anti-$\beta$-actin antibody. (b) Detection of hypermutated genomes by HA-yellow agarose gel electrophoresis. Hypermutated genomes in the presence or absence of APOBEC3G-HA were amplified by 3D-PCR. The white dotted line was added to help visualize the retardation of AT-rich DNA in HA-yellow agarose gel. (c) Quantification analysis of hypermutated genomes by real-time 3D-PCR. Results are means ± SD values of three independent experiments.

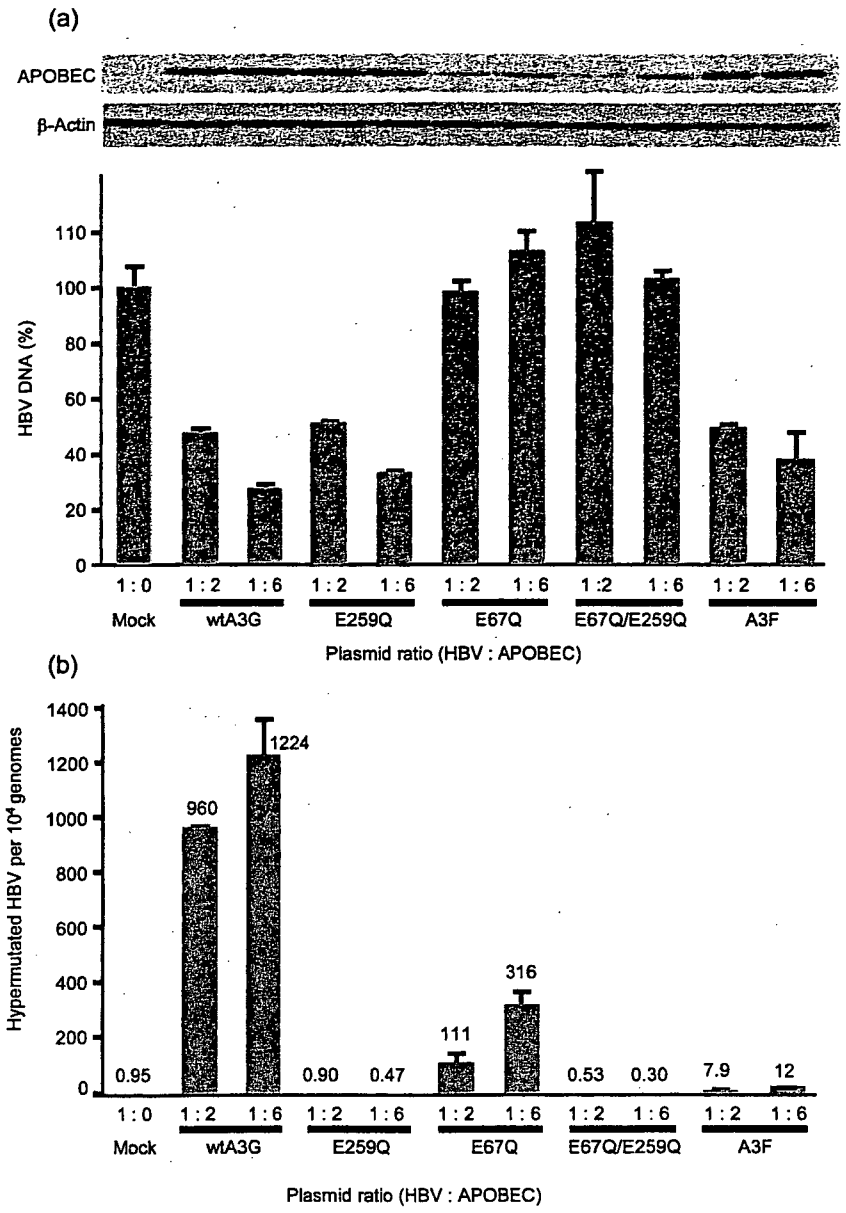


**Fig. 8.** Effect of APOBEC proteins on HBV hypermutation. A plasmid containing 1.4 genome length HBV DNA was co-transfected with wild-type, enzymically impaired APOBEC3G mutants (E67Q, E259Q, E67Q/E259Q) and APOBEC3F into Huh7 cells (plasmid ratio HBV : APOBEC = 1 : 2 or 1 : 6). The cells were harvested at 96 h after transfection. (a) Quantification of core-associated HBV DNA and Western blot analysis of cytoplasmic extracts with anti-HA or anti-β-actin antibody. (b) Quantification of hypermutated genomes by real-time 3D-PCR. Results are means ± SD values of three independent experiments.

APOBEC3G. These results suggest that hypermutation of HBV contributes very little to reduce the number of replicative intermediate.

## DISCUSSION

Induction of G to A hypermutation in HIV has been reported as part of host innate immunity against virus infection (Mangeat *et al.*, 2003; Zhang *et al.*, 2003; Lecossier *et al.*, 2003; Harris *et al.*, 2003; Sheehy *et al.*, 2002). We and others have reported the presence of hypermutated genomes of HBV in serum samples of chronically infected patients and in HepG2 cell lines (Gunther *et al.*, 1997; Suspene *et al.*, 2005a; Noguchi *et al.*, 2005; Rosler *et al.*, 2004). Hypermutation of HBV was induced in hepatocytes (Noguchi *et al.*, 2005), and expression of APOBEC proteins in liver cell-derived cell lines increased hypermutation (Suspene *et al.*, 2005b; Rosler *et al.*, 2004). However, the estimated number of hypermutated genomes in chronically infected patients is very low (Noguchi *et al.*, 2005; Suspene *et al.*, 2005b). The reason for the partial hypermutation of HBV remains an enigma. It might be due to the low expression levels of APOBEC proteins in liver cells (Jarmuz *et al.*, 2002). Alternatively, rapid packaging of pregenome RNA into capsid might prevent access of APOBEC3G to the first strand DNA. Furthermore, rapid degradation of edited HBV genomes by uracil DNA glycosylase in liver cells might also explain the low number of hypermutated genomes.

The mechanism that controls the activities of APOBEC proteins to cause hypermutation has not been analysed until

recently. Tanaka *et al.* (2006) reported that IFN-α increases the expression levels of APOBEC3G mRNA. They reported the presence of ISRE elements in the promoter region of APOBEC3G and that the promoter was activated by IFN-α. However, they did not examine the occurrence of G to A hypermutation in their experiments. Moreover, Peng *et al.* (2006) showed that IFN-α and -γ cooperatively induce APOBEC3G expression and that the inhibition of HIV production by a small number of IFN is cancelled by a small interfering RNA (siRNA) against APOBEC3G. More recently, Bonvin *et al.* (2006) demonstrated that IFN-α induces transcription of APOBEC proteins. They showed that IFN treatment increased APOBEC3B, -3C, -3F and -3G mRNAs, particularly when they used primary cultured hepatocytes. They also reported that they were able to detect hypermutated genomes after transfection of APOBEC3 plasmids, but did not measure the direct effect of IFN on G to A hypermutation.

These studies did not analyse quantitatively the increase in hypermutation of viral genomes. The studies that analysed the expression of APOBEC protein and reduction of HBV DNA also did not analyse quantitatively the number of hypermutated genome (Suspene *et al.*, 2005a; Noguchi *et al.*, 2005; Turelli *et al.*, 2004a, b; Rosler *et al.*, 2005). In the present study, we developed a method that accurately measures the level of hypermutation using real-time PCR. It is often difficult to design a primer set and a probe to detect G to A hypermutation because they are located in a region with many G residues, but the primer and probe sequences should not contain any. It is thus possible that we did not see any C to T substitution because we did not design a primer–probe set to detect this substitution. We also tried to select such a primer–probe set applicable for all genotypes of HBV, but were able to select only one suitable for genotype C.

Using this method, we demonstrated that both IFN-α and -γ increased G to A hypermutation of the HBV genome. Although the expression levels of APOBEC3G increased after IFN treatment, we did not observe an apparent shift of preferred dinucleotide sequence of APOBEC proteins from 3F to 3G. This is probably because the increase in APOBEC3G is only slight (Fig. 5).

The exact mechanism by which IFNs activate the transcription of APOBEC3G is unknown. Furthermore, what kind of sensor(s) detects HBV infection and how the signal is communicated for the production of IFNs and subsequent induction of effector molecules have not been analysed yet. Although the importance of the IFN system in eliminating HBV and its possible mechanism have been reported (Wieland *et al.*, 2004a, b, 2005), further studies are needed to fully describe the mechanism of action of IFNs including the activation of APOBEC3G.

We also demonstrated that the number of hypermutated genomes increased with the expression of APOBEC3G and APOBEC3F (Fig. 8), but not in deaminase-inactive mutants, as demonstrated previously in HIV studies (Shindo *et al.*, 2003; Newman *et al.*, 2005). However, these mutants also reduced the replication of HBV almost to the wild-type level. This suggests that the contribution of hypermutation of HBV to the reduction of virus replication is only minimal and supports the previous report that showed that APOBEC3G reduced the replication of HBV through inhibition of packaging of the pregenome (Turelli *et al.*, 2004a). However, the effect of hypermutation on infectivity of the virus should be investigated further. The effects of APOBEC proteins, including other family members, especially under physiological conditions, should also be examined further. Whether any HBV protein inhibits deamination of the genomic DNA awaits further investigation. Furthermore, the mechanism that enables HBV to cause chronic infection, especially escape from innate antiviral immunity, should also be clarified in order to control chronic HBV infection and reduce HBV-related morbidity.

## ACKNOWLEDGEMENTS

This work was carried out at the Research Center for Molecular Medicine, Faculty of Medicine, Hiroshima University. The authors thank Kana Kunihiro, Asako Kozono, Hiromi Ishino, Rie Akiyama, Eiko Miyoshi and Kiyomi Toyota for the excellent technical assistance, and Yoshiko Nakata for the secretarial assistance. This work was supported in part by a Grant-in-Aid for Scientific Research and development from the Ministry of Education, Sports, Culture and Technology and the Ministry of Health, Labour and Welfare.

## REFERENCES

**Abu-Daya, A., Brown, P. M. & Fox, K. R. (1995).** DNA sequence preferences of several AT-selective minor groove binding ligands. *Nucleic Acids Res* **23**, 3385–3392.

**Bonvin, M., Achermann, F., Greeve, I., Stroka, D., Keogh, A., Inderbitzin, D., Candinas, D., Sommer, P., Wain-Hobson, S. & other authors (2006).** Interferon-inducible expression of APOBEC3 editing enzymes in human hepatocytes and inhibition of hepatitis B virus replication. *Hepatology* **43**, 1364–1374.

**Bruix, J. & Llovet, J. M. (2003).** Hepatitis B virus and hepatocellular carcinoma. *J Hepatol* **39** (Suppl. 1), S59–S63.

**Colonna, M., Krug, A. & Cella, M. (2002).** Interferon-producing cells: on the front line in immune responses against pathogens. *Curr Opin Immunol* **14**, 373–379.

**Ganem, D. & Schneider, R. (2001).** *Hepadnaviridae*: the viruses and their replication. In *Fields Virology*, 4th edn, pp. 2923–2969. Edited by D. M. Knipe & P. M. Howley. Baltimore: Lippincott Williams & Wilkins.

**Ganem, D. & Prince, A. M. (2004).** Hepatitis B virus infection - natural history and clinical consequences. *N Engl J Med* **350**, 1118–1129.

**Grandvaux, N., tenOever, B. R., Servant, M. J. & Hiscott, J. (2002).** The interferon antiviral response: from viral invasion to evasion. *Curr Opin Infect Dis* **15**, 259–267.

**Gunther, S., Sommer, G., Plikat, U., Iwanska, A., Wain-Hobson, S., Will, H. & Meyerhans, A. (1997).** Naturally occurring hepatitis B virus genomes bearing the hallmarks of retroviral G→A hypermutation. *Virology* **235**, 104–108.

**Harris, R. S., Bishop, K. N., Sheehy, A. M., Craig, H. M., Petersen-Mahrt, S. K., Watt, I. N., Neuberger, M. S. & Malim, M. H. (2003).** DNA deamination mediates innate immunity to retroviral infection. *Cell* **113**, 803–809.

**Janini, M., Rogers, M., Birx, D. R. & McCutchan, F. E. (2001).** Human immunodeficiency virus type 1 DNA sequences genetically damaged by hypermutation are often abundant in patient peripheral blood mononuclear cells and may be generated during near-simultaneous infection and activation of CD4(+) T cells. *J Virol* **75**, 7973–7986.

**Jarmuz, A., Chester, A., Bayliss, J., Gisbourne, J., Dunham, I., Scott, J. & Navaratnam, N. (2002).** An anthropoid-specific locus of orphan C to U RNA-editing enzymes on chromosome 22. *Genomics* **79**, 285–296.

**Kobayashi, M., Takaori-Kondo, A., Shindo, K., Abudu, A., Fukunaga, K. & Uchiyama, T. (2004).** APOBEC3G targets specific virus species. *J Virol* **78**, 8238–8244.

**Lecossier, D., Bouchonnet, F., Clavel, F. & Hance, A. J. (2003).** Hypermutation of HIV-1 DNA in the absence of the Vif protein. *Science* **300**, 1112.

**Mangeat, B., Turelli, P., Caron, G., Friedli, M., Perrin, L. & Trono, D. (2003).** Broad antiretroviral defence by human APOBEC3G through lethal editing of nascent reverse transcripts. *Nature* **424**, 99–103.

**Newman, E. N., Holmes, R. K., Craig, H. M., Klein, K. C., Lingappa, J. R., Malim, M. H. & Sheehy, A. M. (2005).** Antiviral function of APOBEC3G can be dissociated from cytidine deaminase activity. *Curr Biol* **15**, 166–170.

**Noguchi, C., Ishino, H., Tsuge, M., Fujimoto, Y., Imamura, M., Takahashi, S. & Chayama, K. (2005).** G to A hypermutation of hepatitis B virus. *Hepatology* **41**, 626–633.

**Norder, H., Courouce, A. M. & Magnius, L. O. (1994).** Complete genomes, phylogenetic relatedness, and structural proteins of six strains of the hepatitis B virus, four of which represent two new genotypes. *Virology* **198**, 489–503.

**Peng, G., Lei, K. J., Jin, W., Greenwell-Wild, T. & Wahl, S. M. (2006).** Induction of APOBEC3 family proteins, a defensive maneuver underlying interferon-induced anti-HIV-1 activity. *J Exp Med* **203**, 41–46.

**Rosler, C., Kock, J., Malim, M. H., Blum, H. E. & von Weizsacker, F. (2004).** Comment on 'Inhibition of hepatitis B virus replication by APOBEC3G'. *Science* **305**, 1403 (author reply 1403).

**Rosler, C., Kock, J., Kann, M., Malim, M. H., Blum, H. E., Baumert, T. F. & von Weizsacker, F. (2005).** APOBEC-mediated interference with hepadnavirus production. *Hepatology* **42**, 301–309.

**Samuel, C. E. (2001).** Antiviral actions of interferons. *Clin Microbiol Rev* **14**, 778–809.

**Seeger, C. & Mason, W. S. (2000).** Hepatitis B virus biology. *Microbiol Mol Biol Rev* **64**, 51–68.

**Sheehy, A. M., Gaddis, N. C., Choi, J. D. & Malim, M. H. (2002).** Isolation of a human gene that inhibits HIV-1 infection and is suppressed by the viral Vif protein. *Nature* **418**, 646–650.

**Shindo, K., Takaori-Kondo, A., Kobayashi, M., Abudu, A., Fukunaga, K. & Uchiyama, T. (2003).** The enzymatic activity of CEM15/Apobec-3G is essential for the regulation of the infectivity of HIV-1 virion but not a sole determinant of its antiviral activity. *J Biol Chem* **278**, 44412–44416.

**Shirakawa, K., Takaori-Kondo, A., Kobayashi, M., Tomonaga, M., Izumi, T., Fukunaga, K., Sasada, A., Abudu, A., Miyauchi, Y. & other authors (2006).** Ubiquitination of APOBEC3 proteins by the Vif-Cullin5-ElonginB-ElonginC complex. *Virology* **344**, 263–266.

**Skalka, A. M. & Goff, S. P. (1993).** *Reverse Transcriptase.* Cold Spring Harbor, NY: Cold Spring Harbor Laboratory Press.

**Summers, J. & Mason, W. S. (1982).** Replication of the genome of a hepatitis B-like virus by reverse transcription of an RNA intermediate. *Cell* **29**, 403–415.

**Suspene, R., Guetard, D., Henry, M., Sommer, P., Wain-Hobson, S. & Vartanian, J. P. (2005a).** Extensive editing of both hepatitis B virus DNA strands by APOBEC3 cytidine deaminases in vitro and in vivo. *Proc Natl Acad Sci U S A* **102**, 8321–8326.

**Suspene, R., Henry, M., Guillot, S., Wain-Hobson, S. & Vartanian, J. P. (2005b).** Recovery of APOBEC3-edited human immunodeficiency virus G→A hypermutants by differential DNA denaturation PCR. *J Gen Virol* **86**, 125–129.

**Tanaka, Y., Marusawa, H., Seno, H., Matsumoto, Y., Ueda, Y., Kodama, Y., Endo, Y., Yamauchi, J., Matsumoto, T. & other authors (2006).** Anti-viral protein APOBEC3G is induced by interferon-α stimulation in human hepatocytes. *Biochem Biophys Res Commun* **341**, 314–319.

**Tsuge, M., Hiraga, N., Takaishi, H., Noguchi, C., Oga, H., Imamura, M., Takahashi, S., Iwao, E., Fujimoto, Y. & other authors (2005).** Infection of human hepatocyte chimeric mouse with genetically engineered hepatitis B virus. *Hepatology* **42**, 1046–1054.

**Turelli, P., Jost, S., Mangeat, B. & Trono, D. (2004a).** Response to comment of 'Inhibition of hepatitis B virus replication by APOBEC3G'. *Science* **305**, 1403b.

**Turelli, P., Mangeat, B., Jost, S., Vianin, S. & Trono, D. (2004b).** Inhibition of hepatitis B virus replication by APOBEC3G. *Science* **303**, 1829.

**Wieland, S., Thimme, R., Purcell, R. H. & Chisari, F. V. (2004a).** Genomic analysis of the host response to hepatitis B virus infection. *Proc Natl Acad Sci U S A* **101**, 6669–6674.

**Wieland, S. F., Spangenberg, H. C., Thimme, R., Purcell, R. H. & Chisari, F. V. (2004b).** Expansion and contraction of the hepatitis B virus transcriptional template in infected chimpanzees. *Proc Natl Acad Sci U S A* **101**, 2129–2134.

**Wieland, S. F., Eustaquio, A., Whitten-Bauer, C., Boyd, B. & Chisari, F. V. (2005).** Interferon prevents formation of replication-competent hepatitis B virus RNA-containing nucleocapsids. *Proc Natl Acad Sci U S A* **102**, 9913–9917.

**Wright, T. L. & Lau, J. Y. (1993).** Clinical aspects of hepatitis B virus infection. *Lancet* **342**, 1340–1344.

**Zhang, H., Yang, B., Pomerantz, R. J., Zhang, C., Arunachalam, S. C. & Gao, L. (2003).** The cytidine deaminase CEM15 induces hypermutation in newly synthesized HIV-1 DNA. *Nature* **424**, 94–98.

PO Box 2345, Beijing 100023, China
www.wjgnet.com
wjg@wjgnet.com

World J Gastroenterol 2007 January 21; 13(3): 414-420
World Journal of Gastroenterology ISSN 1007-9327


RAPID COMMUNICATION

# Clinical features and prognosis of patients with extrahepatic metastases from hepatocellular carcinoma

Kiminori Uka, Hiroshi Aikata, Shintaro Takaki, Hiroo Shirakawa, Soo Cheol Jeong, Keitaro Yamashina, Akira Hiramatsu, Hideaki Kodama, Shoichi Takahashi, Kazuaki Chayama

Kiminori Uka, Hiroshi Aikata, Shintaro Takaki, Hiroo Shirakawa, Soo Cheol Jeong, Keitaro Yamashina, Akira Hiramatsu, Hideaki Kodama, Shoichi Takahashi, Kazuaki Chayama, Department of Medicine and Molecular Science, Division of Frontier Medical Science, Programs for Biomedical Research, Graduate School of Biomedical Sciences, Hiroshima University, Hiroshima, Japan
Correspondence to: Kiminori Uka, MD, Department of Medicine and Molecular Science, Division of Frontier Medical Science, Programs for Biomedical Research, Graduate School of Biomedical Sciences, Hiroshima University, 1-2-3 Kasumi, Minami-ku, Hiroshima 734-8551, Japan. kiminori@hiroshima-u.ac.jp
Fax: +81-82-2575194
Received: 2006-10-29 Accepted: 2006-12-08

## Abstract

**AIM:** To assess the clinical features and prognosis of 151 patients with extrahepatic metastases from primary hepatocellular carcinoma (HCC), and describe the treatment strategy for such patients.

**METHODS:** After the diagnosis of HCC, all 995 consecutive HCC patients were followed up at regular intervals and 151 (15.2%) patients were found to have extrahepatic metastases at the initial diagnosis of primary HCC or developed such tumors during the follow-up period. We assessed their clinical features, prognosis, and treatment strategies.

**RESULTS:** The most frequent site of extrahepatic metastases was the lungs (47%), followed by lymph nodes (45%), bones (37%), and adrenal glands (12%). The cumulative survival rates after the initial diagnosis of extrahepatic metastases at 6, 12, 24, and 36 mo were 44.1%, 21.7%, 14.2%, 7.1%, respectively. The median survival time was 4.9 mo (range, 0-37 mo). Fourteen patients (11%) died of extrahepatic HCC, others died of primary HCC or liver failure.

**CONCLUSION:** The prognosis of HCC patients with extrahepatic metastases is poor. With regard to the cause of death, many patients would die of intrahepatic HCC and few of extrahepatic metastases. Although most of HCC patients with extrahepatic metastases should undergo treatment for the primary HCC mainly, treatment of extrahepatic metastases in selected HCC patients who have good hepatic reserve, intrahepatic tumor stage (T0-T2), and are free of portal venous invasion may improve survival.



**Key words:** Hepatocellular carcinoma; Extrahepatic metastases; Prognosis; Causes of death

Uka K, Aikata H, Takaki S, Shirakawa H, Jeong SC, Yamashina K, Hiramatsu A, Kodama H, Takahashi S, Chayama K. Clinical features and prognosis of patients with extrahepatic metastases from hepatocellular carcinoma. *World J Gastroenterol* 2007; 13(3): 414-420

http://www.wjgnet.com/1007-9327/13/414.asp

## INTRODUCTION

Hepatocellular carcinoma (HCC) is a highly malignant tumor with frequent intrahepatic metastasis. The prognosis of HCC patients has improved because of progress in therapeutic procedures, such as surgical resection, radiofrequency ablation (RFA), percutaneous ethanol injection (PEI), and transcatheter arterial chemoembolization (TACE)[1-3]. Moreover, progress in diagnostic modalities, such as ultrasonography (US), computed tomography (CT), magnetic resonance imaging (MRI), and digital subtraction angiography (AG) has led to a better detection of patients with early and small HCC or asymptomatic extrahepatic metastases.

The above improvements in survival and diagnostic modalities have resulted in increased detection of extrahepatic metastases from primary HCC and further increases are anticipated in the future. Several groups have investigated extrahepatic metastases from HCC, but many of such cases were in autopsy cases, in a small number of cases or case reports[4-15]. At present, the prognosis of patients with extrahepatic metastases from primary HCC is poor[16,17]. In this regard, there is only little information about the causes of death of such patients[18], and there is no consensus on the treatment strategy for extrahepatic metastases from HCC. For example, what treatment strategy should be used to treat intrahepatic HCC or extrahepatic metastases? Among patients with extrahepatic metastases from primary HCC, which patients should be treated? To our knowledge, there are no reports that

deal directly with these questions. In this relatively large study, we retrospectively assessed the clinical features and prognosis of 151 patients with extrahepatic metastases from primary HCCs, and described the treatment strategy for such patients.

## MATERIALS AND METHODS

### Patients

From June 1990 to December 2005, 995 consecutive patients with HCC were admitted to our hospital. Among these patients, 880 were initially diagnosed with HCC in our hospital while the others were treated previously for HCC in other hospitals. Extrahepatic metastases from primary HCC were detected in 151 (15.2%) of 995 patients. None of the patients was treated for extrahepatic metastases. All the 151 HCC patients with extrahepatic metastases (117 men and 34 women, median age: 64 years, range: 21-82 years) were enrolled in the present study.

Table 1 summarizes the clinical profile of the 151 patients at the initial diagnosis of extrahepatic metastases. These 151 patients were divided into groups A and B. Group A was consisted of 68 patients presented with extrahepatic metastases together with primary HCC at the initial diagnosis of HCC, group B was composed of 83 patients who received treatment for intrahepatic HCC, and developed extrahepatic metastases during the follow-up period. Among them, 37 (25%) patients were treated previously for primary HCC in other hospitals, 90 patients were of performance status (PS) of 0, 43 patients of 1, 9 patients of 2, 6 patients of 3, and 3 patients of 4[19]. The etiology of the background liver disease was hepatitis B virus (HBV) in 33 patients, hepatitis C virus (HCV) in 89 patients, HBV and HCV in 5 patients, and non-B non-C in 24 patients. The hepatic reserve was Child-Pugh grade A in 88 patients, grade B in 48 patients, and grade C in 15 patients. We evaluated the primary tumor stage according to the Liver Cancer Study Group of Japan criteria[20], based on the following three conditions (T factor): solitary, < 2 cm in diameter, and no vessel invasion. T1 was defined as fulfilling the three conditions, T2 as fulfilling two of the three conditions, T3 as fulfilling one of the three conditions, T4 as fulfilling none of the three conditions. The primary HCC tumor stage at the first diagnosis of extrahepatic metastases was T0 (no intrahepatic HCC) in 11 (7%) patients, T1 in 4 (3%) patients, T2 in 13 (9%) patients, T3 in 43 (28%) patients, and T4 in 80 (53%) patients. Twenty seven of 28 patients with intrahepatic tumor stage T0-T2 were treated previously for intrahepatic HCC. The median size of the main intrahepatic primary tumor was 48 mm (range, 0-160 mm). Intrahepatic tumor morphology was nodular type in 83 (55%) patients, non-nodular type in 57 (38%) patients, and no intrahepatic HCC in 11 (7%) patients. Table 1 lists the sites of extrahepatic metastases at enrollment. Among the 151 patients with extrahepatic metastases, the sites of metastases were the lungs in 63 patients, lymph nodes in 60 patients, bones in 51 patients, adrenal glands in 16 patients and other locations (e.g., peritoneum, pancreas and nasal passages). In some patients, two or more distant metastatic tumors were found in one or more organs.

**Table 1 Clinical profile of 151 HCC patients with extrahepatic metastases at the initial diagnosis of extrahepatic metastases**

| | |
|---|---|
| Age (yr) | 64 (21-82) |
| Sex (male/female) | 117/34 |
| Etiology (HBV/HCV/HBV + HCV/others) | 33/89/5/24 |
| PS (0/1/2/3/4) | 90/43/9/6/3 |
| Intrahepatic tumor stage (T0/1/2/3/4) | 11/4/13/43/80 |
| Intrahepatic main tumor size (mm) | 48 (0-160) |
| Intrahepatic tumor volume (< 50%/≥ 50%) | 103/48 |
| Intrahepatic tumor morphology (nodular type/non nodular type/no intrahepatic HCC) | 83/57/11 |
| Grade of portal vein invasion (Vp 0/1/2/3/4) | 74/0/26/28/23 |
| Child-Pugh grade (A/B/C) | 88/48/15 |
| AFP (ng/mL) | 741.8 (< 5-861600) |
| DCP (mAU/mL) | 1300 (< 10-391400) |
| Site of extrahepatic metastases, *n* (%) | |
| Lung | 63 (42) |
| Lymph nodes | 60 (40) |
| Bone | 51 (34) |
| Adrenal | 16 (11) |
| Peritoneum | 1 (0.7) |
| Pancreas | 1 (0.7) |
| Nasal passages | 1 (0.7) |

Data are expressed as medians and ranges unless indicated otherwise. HBV: hepatitis B virus; HCV: hepatitis C virus; PS: Eastern Cooperative Oncology Group performance status; T0: no intrahepatic HCC; Portal invasion assessed Vp1: tumor thrombus in a third or more of the peripheral branches; Vp2: in the second branch; Vp3: in the first branch; Vp4: in the trunk; AFP: alpha-fetoprotein; DCP: Des-γ-carboxy prothrombin.

### Hepatocellular carcinoma

A definitive diagnosis of HCC was based on the finding of typical hypervascular radiological features or histopathological examination of needle biopsy specimen. HCC was also assessed by US, CT, and/or AG. Furthermore, CT was obtained during arterial portography and computerized tomographic hepatic arteriography. Further assessment of HCC was conducted by measuring α-fetoprotein (AFP) and des-γ-carboxy prothrombin (DCP).

Extrahepatic metastases were diagnosed by CT, MRI, bone scintigraphy, X-ray, and/or positron emission tomography (PET) with $^{18}$F-fluorodeoxyglucose (FDG), or diagnosed by histopathological examination of surgically resected specimen or biopsy. When we suspected extrahepatic metastases with HCC, we always ruled out other malignancies (such as gastric cancer, colon cancer and lung cancer) by several imaging modalities, serological tumor markers and/or pathological examination.

### Follow- up

All the 151 HCC patients with extrahepatic metastases were followed up during the observation period and no one was lost to follow-up. The median follow-up period was 4.9 mo (range, 1-37 mo). After the diagnosis of HCC, all patients were screened at regular intervals for the development of intra/extra hepatic metastases by clinical examination, AFP, DCP, and/or various imaging modalities. Serological tumor markers were measured once every month. US, CT or MRI was performed once every three to six months.

### Statistical analysis and ethical considerations

Differences between groups were examined for statistical significance using the Mann-Whitney test (*U*-test) and $\chi^2$ test where appropriate. Cumulative survival rate was assessed by the Kaplan-Meier life-table method and the differences were evaluated by the log rank test. The following 15 potential predictors were assessed in this study: PS (0 *vs* 1-4), age (≤ 65 *vs* > 65 years), sex (M *vs* F), Child-Pugh stage (A *vs* B, C), intrahepatic tumor stage (T0-T2 *vs* T3, T4), main intrahepatic tumor size (≤ 50 *vs* > 50 mm), intrahepatic tumor volume (≤ 50% *vs* > 50%), intrahepatic tumor morphology (nodular type *vs* non nodular type), portal venous invasion (Vp 0-2 *vs* > Vp 3, 4), AFP (≤ 400 ng/mL *vs* > 400 ng/mL), DCP (≤ 1000 mAU/mL *vs* > 1000 mAU/mL), site of extrahepatic metastases (lung *vs* others, bone *vs* others, only lymph node *vs* others), and treatment for extrahepatic metastases (performed *vs* not performed). All factors that were at least marginally associated with the survival after diagnosis of extrahepatic metastases ($P < 0.05$) were entered into a multivariate analysis. The hazard ratio and 95% confidence interval (95% CI) were calculated to assess the relative risk confidence. All analyses described above were performed using the SPSS program (version 11.0, SPSS Inc., Chicago, IL).

The study protocol was approved by the Human Ethics Review Committee of Graduate School of Biomedical Sciences, Hiroshima University and a signed consent form was obtained from each patient.

## RESULTS

### Site of extrahepatic metastases

Table 2 lists the sites of extrahepatic metastases identified throughout the follow-up period. The most frequent site of metastases that were identified throughout the follow-up period was the lung ($n$ = 71 patients, 47%), followed by lymph nodes ($n$ = 68 patients, 45%), bone ($n$ = 56 patients, 37%), and adrenal glands ($n$ = 18 patients, 12%). Brain metastases were identified in 2 (1%) patients. One (0.7%) patient each had metastases in the peritoneum, pancreas, nasal passages, muscle, skin, diaphragm, and colon. Autopsy was performed in 14 cases with metastases. Despite the detection of extrahepatic metastases in these 14 patients before autopsy, additional extrahepatic metastases were detected on postmortem examination (lymph nodes, diaphragm, and colon). At the first diagnosis of extrahepatic metastases, 109 (72%) patients had single-organ metastases, while the others had multiple organ metastases.

Among the 71 patients with lung metastases, 23 patients had bilateral lung metastases, 14 had additional extrapulmonary site of metastatic disease. The size of pulmonary nodules ranged from 9 to 30 mm at initial diagnosis of extrahepatic HCC. Few patients had symptoms (cough, dyspnea, and pleural effusion) related to lung metastases, and 8 patients who had severe symptoms died subsequently of respiratory failure. The median survival period of these 8 patients was 4.3 mo (range, 2.5-14.4 mo).

**Table 2 Sites of extrahepatic HCC detected throughout the entire follow-up period**

| Site | Patients ($n$ = 151), $n$ (%) |
|---|---|
| Lung | 71 (47) |
| Lymph nodes | 68 (45) |
| Bone | 56 (37) |
| Adrenal | 18 (12) |
| Brain | 2 (1) |
| Peritoneum | 1 (0.7) |
| Pancreas | 1 (0.7) |
| Nasal | 1 (0.7) |
| Muscle | 1 (0.7) |
| Skin | 1 (0.7) |
| Diaphragm | 1 (0.7) |
| Colon | 1 (0.7) |

Among the 68 patients with lymph node metastases, metastases were identified in 64 regional lymph nodes. The most common site was in the paraaortic nodes (31/64), followed by portohepatic nodes (21/64), periceliac nodes (6/64) and peripancreatic nodes (6/64). The majority of patients with regional lymph nodes metastases were asymptomatic, but few regional lymph nodes (portohepatic nodes) caused obstructive jaundice. Distant nodal metastases were found at 17 sites. The most common site was the mediastinum nodes (10/17), followed by subclavicular nodes (3/17), iliac nodes (2/17), cardiophrenic node (1/17), and retrocrural node (1/17). All distant lymph node metastases were not associated with clinical symptoms in this study.

Fifteen of 56 patients with bone metastases had multiple bone metastases at the initial diagnosis of bone metastases. The total number of bone metastatic sites was 88. The most frequent site was the vertebra (63/88; cervical vertebrae = 9, thoracic vertebrae = 38, and lumbar vertebrae = 16), followed by the ribs (8/88). Bone metastases were diagnosed by CT, MRI, bone scintigraphy, and/or PET with FDG.

Of the 18 patients with adrenal gland metastases, 13 had right adrenal gland metastases, 4 had left adrenal gland metastases and only one patient had bilateral metastases. These metastases were not associated with symptoms.

### Treatments of extrahepatic metastases

All patients with Child-Pugh grade other than C or PS other than 2-4 were treated for intrahepatic HCC, and many of them were continuously treated after the diagnosis of extrahepatic metastases. On the other hand, HCC patients with Child-Pugh grade C or PS of 2-4 received supportive care. Forty-nine (32%) of 151 patients were treated for extrahepatic metastases by surgical resection, TACE, systemic chemotherapy, and/or radiotherapy. The 49 patients had extrahepatic metastases that were considered to worsen prognosis.

Surgical resection was performed in three (2%) patients (with regional lymph node, adrenal gland and lung metastases). The survival periods after surgical resection of extrahepatic metastases were 7 mo (in patients with lymph node metastases), 23 mo (in patients adrenal gland metastases), and 37 mo (in patients with lung metastases).

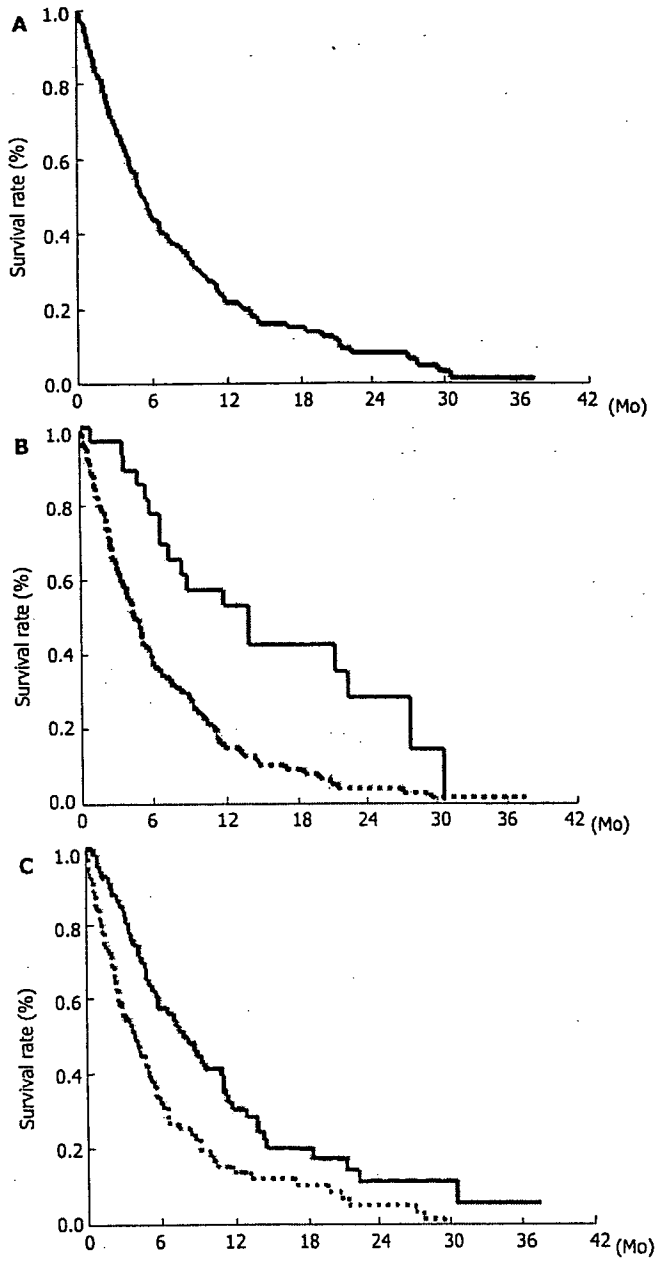


**Figure 1** Survival rate of 151 HCC patients with extrahepatic metastases (A), intrahepatic tumor stage (B) [solid line: T0-T2, dashed line: T3, T4 (log-rank test: $P < 0.001$)], and after treatment of extrahepatic metastases (C) [solid line: treatment group, dashed line: no treatment group (log-rank test: $P < 0.001$)].

These three were all alive without recurrence of extrahepatic metastases during the observation period. In each of these 3 patients, hepatic reserve was Child-Pugh stage A, no intrahepatic HCC was not detected, and PS was 0.

TACE was performed in 8 (5%) patients (7 patients with adrenal gland metastases, and one patient with paraaortic lymph node metastases). Systemic chemotherapy was used in 39 (26%) patients. Chemotherapy included 5-fluorouracil, carboplatin, cisplatin. Twenty-five of the 39 patients had lung metastases, 10 had lymph node metastases, 2 had bone metastases, one had lung and lymph node metastases, and one had lung, adrenal gland and lymph node metastases.

Radiotherapy was performed in 36 (24%) patients.

**Table 3 Univariate analysis of predictors of survival after initial diagnosis of extrahepatic metastases in 151 patients**

| Variable | Hazard Ratio | 95% CI | *P* |
|---|---|---|---|
| PS (0 *vs* 1-4) | 2.181 | 1.50-3.17 | < 0.001 |
| Age (≤ 65 *vs* > 65 yr) | 0.988 | 0.97-1.0 | 0.18 |
| Sex (M *vs* F) | 0.889 | 0.57-1.38 | 0.601 |
| Child Pugh stage (A *vs* B, C) | 2.323 | 1.73-3.12 | < 0.001 |
| Intrahepatic main tumor size (≤ 50 *vs* > 50 mm) | 2.321 | 1.52-3.54 | < 0.001 |
| Intrahepatic tumor volume (≤ 50 *vs* > 50%) | 2.523 | 1.71-3.72 | < 0.001 |
| Intrahepatic tumor morphology (nodular *vs* non nodular) | 1.506 | 1.04-2.18 | 0.03 |
| Vp (0-2 *vs* 3, 4) | 2.247 | 1.53-3.29 | < 0.001 |
| AFP (≤ 400 *vs* > 400 ng/mL) | 1.158 | 0.80-1.68 | 0.439 |
| DCP (≤ 1000 *vs* > 1000 mAU/mL) | 1.584 | 1.08-2.33 | 0.02 |
| Treatment (performed *vs* not performed)[1] | 2.385 | 1.51-3.77 | < 0.001 |
| Site (lung *vs* others)[2] | 1.065 | 0.74-1.52 | 0.731 |
| Site (bone *vs* others) | 1.61 | 1.11-2.33 | 0.012 |
| Site (only lymph node *vs* others) | 1.133 | 0.74-1.74 | 0.567 |

[1]Treatments: various treatments for extrahepatic metastases (surgical resection, TACE, systemic chemotherapy and/or radiotherapy); [2]Site: site of extrahepatic metastases.

Curative therapy was performed in 10 patients (6 patients with lymph node metastases and 4 patients with adrenal gland metastases). Palliative therapy was performed in the remaining 26 patients who had severe pain due to bone metastases. Furthermore, 9 patients with painful bone metastases were treated with RFA therapy combined with cementoplasty[21]. Nonsteroidal anti-inflammatory drugs or opioids were used in patients with bone metastases due to severe pain.

### *Survival data*

The cumulative survival rates of the 151 HCC patients with extrahepatic metastases after initial diagnosis of extrahepatic metastases at 6, 12, 24, and 36 mo were 44.1%, 21.7%, 14.2%, and 7.1%, respectively (Figure 1A). The median survival period was 4.9 mo (range, 1-37 mo). Survival was compared among patients with intrahepatic tumor stage T0-T2 and T3, T4 (Figure 1B). The rate was significantly higher in the intrahepatic tumor stage T0-T2 groups than in the T3, T4 groups ($P < 0.001$). We investigated the determinants of survival after initial diagnosis of extrahepatic metastases. Univariate analysis identified the following 9 factors significantly influencing survival: PS, 0 ($P < 0.001$); Child-Pugh grade, A ($P < 0.001$); intrahepatic main tumor size, < 50 mm ($P < 0.001$); intrahepatic tumor volume, < 50% ($P < 0.001$); portal venous invasion, Vp 0-2 ($P < 0.001$); use of treatment for extrahepatic metastases ($P < 0.001$, Figure 1C); bone metastasis ($P = 0.012$); DCP < 1000 mAU/mL ($P = 0.02$); and nodular type intrahepatic tumor ($P = 0.03$) (Table 3). Since the variables could be mutually correlated, multivariate analysis was performed. The analysis identified the following four variables as significant and independent determinants of survival after initial diagnosis of extrahepatic metastases: PS ($P < 0.001$), portal venous invasion ($P < 0.001$), treatment of extrahepatic metastases ($P = 0.003$), and Child-Pugh grade ($P = 0.009$) (Table 4).